1.E.1:3.A *Nuclear Physics* A197 (1972) 129—162; © *North-Holland Publishing Co., Amsterdam*

^{116}In LEVEL SCHEME AND p-n CONFIGURATIONS

D. RABENSTEIN, D. HARRACH and H. VONACH
Physik-Department der Technischen Universität München, 8046 Garching, Lichtenbergstr., Fed. Rep. of Germany
G. G. DUSSEL † and R. P. I. PERAZZO †
CNEA Ciclotron, Av. del Libertador 8250, Buenos Aires, Argentina

Received 4 August 1972

Abstract: The low-energy and high-energy γ-ray spectra associated with the reaction ^{115}In(n, γ)^{116}In have been measured with Ge(Li) detectors and a Ge(Li)-NaI(Tl) pair spectrometer. A γ-γ coincidence study has been performed using a Ge(Li)-Ge(Li) coincidence system. Combining these measurements with the results of (d, p) and other (n, γ) studies, a level scheme for ^{116}In up to 1.4 MeV is proposed. In particular, seven states of the $(\pi(g_{\frac{9}{2}})^{-1}, \nu h_{\frac{11}{2}})$ multiplet (3^- to 9^-) are unambiguously identified and the anomalous high isomeric cross-section ratio of the second isomeric state is explained. The binding energy B_n of the last neutron in ^{116}In has been determined to be 6784.2 ± 1.2 keV. From the energy splitting of the fairly pure high-spin states of the $(\pi(g_{\frac{9}{2}})^{-1}, \nu h_{\frac{11}{2}})$ multiplet, the coupling constant of the quadrupole part of the residual proton-neutron interaction κ_2 is calculated in a spherical basis. The κ_2 obtained is about 5 times larger than the one normally used in calculations of quadrupole oscillations in doubly even nuclei. This discrepancy is discussed, and an explanation in terms of an isovector component of the quadrupole interaction is proposed.

E NUCLEAR REACTIONS ^{115}In(n, γ), E = th; measured E_γ, I_γ, γ-γ coin; deduced Q. ^{116}In deduced levels, J, π, γ-branching. Natural and enriched targets, Ge(Li) detectors.

1. Introduction

The purpose of the present paper is to study the proton-neutron interaction in nuclei which are far away from closed shells in one type of particle. The low-energy spectra of doubly even systems depend very strongly on the short-range part of the residual interaction. In doubly odd systems, one can determine much more precisely the residual long-range part of the force owing to the appearance of some special levels at low energy. It must be remembered that when one makes a multipole expansion of the force, the short-range part determines the higher multipoles while the long-range part determines the lower multipoles.

Up to now, the doubly odd nuclei theoretically studied [1]) have been mainly the ones near closed shells.

We have chosen for our study the nucleus ^{116}In for several reasons. The first is that the single-particle proton and neutron levels present in that region suggest that there may be several levels (the 1^+, 8^+ and high-spin negative-parity states) that will have

† Fellow of the Consejo Nacional de Investigaciones Cientificas y Tecnicos, Argentina.

a pure structure, namely a $g_{\frac{9}{2}}$ proton hole coupled to a neutron quasiparticle. Another interesting point is that the nuclei ^{115}In and ^{117}In seem to have excited deformed bands which are a puzzle in this spherical zone [2,3]).

In order to complete the experimental information for this nucleus, we have studied the γ-decay after neutron capture in ^{115}In. There has already been considerable interest in the study of ^{116}In by means of the (n, γ) reaction. Measurements of the high-energy transitions are reported in refs. [4-8]). Low-energy γ-transitions have been measured with Ge(Li) detectors [7-9]) and with crystal spectrometers [10,11]). Also, low energy conversion-electron studies [12,13]) and a γ-γ coincidence study with 2 Ge(Li) detectors [14]) have been carried out. Extensive measurements of the decay of the low-lying neutron resonances in ^{116}In can be found in refs. [15-17]).

Although level positions and characteristics have also been studied by the (d, p) reaction [18-20]) and by the excitation of analog states in the reaction ^{115}In(p, n)^{115}Sn [ref. [18])], no complete and satisfying level scheme of ^{116}In has been published yet.

The construction of a consistent level scheme has been especially complicated by the following facts:

(a) the position of both isomeric states was not accurately known;

(b) the level density is rather high even at low excitation energies;

(c) the number of energy-sum relations from cross-over transitions is relatively small owing to the high configuration purity of many low-lying states, and the large spin differences.

2. Experimental procedure

All measurements have been carried out at the end of a neutron guide tube [21]) installed at the FRM. The neutron flux available was about 10^6 n/cm^2 · sec. Low-energy singles spectra have been measured with Ge(Li) detectors of different efficiencies and resolutions. A Ge(Li)-Ge(Li) coincidence system and, for the high-energy measurements, a three-crystal pair spectrometer have been employed; both have been described in ref. [22]). Details about the procedure by which the coincidence information has been stored on a magnetic disc with the help of a PDP-8 computer can be found in ref. [23]).

The targets consisted of 99.999 % pure In of natural isotopic composition in the form of 0.2 or 0.5 mm thick metal foils and of ^{115}In enriched to 99.99 % in the form of In_2O_3 powder in a polyethylene container.

Using both targets, it was possible to identify transitions belonging to ^{114}In. Transitions in ^{116}Sn, to which the ground state and first excited state of ^{116}In decay, were recognized by comparison with the energies and intensities given in ref. [24]).

3. Experimental results

3.1. SPECTRA

A high-energy γ-spectrum taken with the three-crystal pair spectrometer is shown in fig. 1. Table 1 contains the energies and absolute intensities of the high-energy γ-

transitions above 4.5 MeV. They are believed to be all primary transitions, thus establishing energy levels in ^{116}In up to 2.2 MeV. From the energy differences of these primary transitions, level distances could be calculated with a mean energy error about five times smaller than the absolute mean error of the energy of the primary transitions as given in table 1.

For the energy calibration of the γ-rays in table 1, the 7367.73 ± 0.5 keV line from neutron capture in lead [25]) and the γ-line from neutron capture in H (2223.29 ± 0.07 keV) [ref. [26])] have been used.

In the same way as Lone *et al.* [16]), we have chosen $I_\gamma = 8.6$ per 1000 neutron captures as the absolute intensity of the strong 5891 keV line in ^{116}In, which is the weighted average of the values given by Bartholomew and Kinsey [4]) and Groshev *et al.* [5]) for the absolute intensity of this primary transition.

Only relative errors in the intensities are given in table 1; the additional systematic error for absolute intensity values introduced by our calibration should be less than 15 %.

Pair spectrometer measurements of the high-energy transitions have also been carried out by Fubini *et al.* [8]). In their work, many weak transitions are given above 5.6 MeV which we could not find. The sensitivity of our measurement has normally been three to five times better than the intensities of those weak lines which we could not find. Therefore, 14 of the levels below 1 MeV which Fubini *et al.* based on these weak primary transitions have not been accepted by us.

Fig. 2 shows the low-energy γ-spectrum from neutron capture in natural In obtained with a small high-resolution planar detector (400 eV FWHM at 60 keV), and, in the higher-energy part, with a 25 cm^3 five-sided detector.

The measured energies and intensities contained in table 2 may be compared with the results of Alexejev *et al.* [11]), which are given in columns 3 and 4 of the same table.

In order to facilitate the comparison, the relative γ-intensities of the Leningrad group [11]) have been renormalized to give $I_\gamma(162 \text{ keV}) = 147$ per 1000 neutron captures. For the adopted energy and intensity values, only the results of the Leningrad group and our results have been taken into account. Above 400 keV the γ-intensities obtained in our work are systematically lower than the corresponding intensities of the Leningrad group (with $I_\gamma(162 \text{ keV})$ set equal!). Here, therefore, our own intensity values have been adopted instead of averaged values.

For the energy calibration of the low-energy transitions the 121.97 ± 0.03 keV line of ^{57}Co [ref. [26])] and the 661.635 ± 0.076 keV line of ^{137}Cs have been used; for the correction for non-linearity, we used a precision Hg pulser. The results have been checked applying the energy of two ^{116}In lines, 126.370 and 608.346 keV, for the energy calibration, and six other γ-energy values of ref. [11]) (the 61, 155, 186, 273, 434 and 557 keV lines) for the non-linearity correction. Both sets of energy values agreed well within the error limits. The values given in the table are those calculated according to the second method because for them the error was generally smaller.

The efficiencies of the applied Ge(Li) detectors have been determined up to about

TABLE 1

Energies and intensities of primary γ-rays from thermal neutron capture in natural In

No.	This work		Resonance capture [a])		Final state	
	E_γ (keV)	I_γ per 1000 neutrons captured	E_γ (keV)	$\Sigma I_\gamma/E_\gamma{}^3$ [b])	(keV;	J^π)
1	6656.3±1.5	0.17±0.05	6656.0±2.0	0.8±0.3	127.3	5^+
2	6559.4±1.5	0.16±0.04	6559.0±3.0	0.9±0.4	223.3	4^+
			6505.0±3.0	0.5±0.4		
3	6469.9±1.7	0.07±0.02	6471.0±2.0	1.6±0.5	313.5	5^+
4	6410.4±1.4	0.92±0.20	6411.2±6.7	4.1±0.7	373.4	6^-
5	6324.9±1.4	0.71±0.15	6326.3±6.9	4.0±0.8	458.9	5^-
6	6277.4±2.4	0.04±0.02			508.2	3^+
7	6228.6±1.4	0.52±0.11	6230.4±2.6	10.8±1.0	555.0	4^-
8	6134.7±1.3	0.55±0.11	6136.4±4.0	1.9±0.6	648.9	6^+
9	6125.3±1.3	0.17±0.04			658.1	$4^+(3^-)$
			6057.2±4.9	3.5±0.7	728.8	3^-
10	6048.5±1.3	0.45±0.10	6047.6±2.2	5.9±1.1	735.7	$6^\pm$
			6016.6±7.1	1.6±0.7		
			6005.0±1.7	2.9±0.7		
11	5994.2±1.3	0.16±0.05			789.3	6^+, $(5^+, 7^+)$
			5976.0±7.0	2.0±0.9	813.3?	$3^+, 4^+$
12	5891.3±1.2	8.6 ±1.6	5893.8±1.2	16.6±1.2	892.6	4^-
13	5834.6±1.2	0.43±0.09	5835.8±3.1	10.4±1.0	949.3	$5^\pm, 6^-$
14	5811.9±1.3	0.63±0.15			970.3	
15	5806.8±3.5	0.07±0.07			977.5	
16	5776.2±1.3	0.61±0.14			1007.6	$5^\pm$, (4^+)
17	5768.6±1.2	1.43±0.28	5771.1±1.9	6.6±1.1	1015.5	4^+, $(3^\pm)$
18	5752.8±1.2	0.57±0.12			1031.2	$4^\pm$, (5^+)
19	5731.1±1.2	0.57±0.12	5736.2±5.5	3.6±1.1	1052.6	
20	5713.1±1.3	0.30±0.07	5716.1±4.5	8.0±1.0	1070.9	
21	5703.1±1.6	0.16±0.05	5703.0±4.3	6.4±1.4	1081.9	$4^\pm, 5^+$
22	5688.9±1.9	0.10±0.05	5686.0±4.1	3.2±1.1	1094.2	
23	5662.5±1.4	0.15±0.05			1121.5	
24	5617.3±1.4	0.14±0.04			1167.0	
25	5596.3±1.6	0.10±0.04			1187.3	$4^\pm, 5^+$
26	5579.6±1.1	1.30±0.25	5576.0±5.0	4.0±1.4	1204.3	$(5, 6)^\pm$
27	5570.7±1.1	0.86±0.17			1213.4	
28	5532.1±2.0	0.11±0.05			1252.6	
29	5525.1±1.2	0.51±0.11	5528.0±2.0	4.3±1.4	1260.1	
30	5498.3±1.1	1.51±0.28	5502.1±2.1	10.4±1.4	1285.7	$(4, 5, 6)^-$
31	5480.9±1.1	1.02±0.19	5484.5±2.1	3.8±1.4	1304.4	
			5467.2±5.1	2.9±1.4		
32	5442.5±1.1	0.46±0.10	5445.2±3.7	4.5±1.4	1343.5	$4^\pm, 5^\pm$
33	5409.8±1.1	2.52±0.47	5412.0±5.1	15.6±2.3	1374.5	$(4, 5, 6)^-$
34	5384.3±1.4	0.23±0.07	5386.6±2.3	4.7±1.5	1399.7	$4^\pm$
35	5357.7±1.1	2.18±0.40	5360.8±2.0	5.9±1.7	1426.4	
36	5346.3±1.1	1.85±0.35	5349.4±2.1	6.2±1.4	1437.7	
37	5332.5±1.1	3.80±0.70	5335.8±2.2	7.4±1.5	1451.1	$(4, 5)^\pm$
38	5318.2±1.1	1.62±0.31	5320.6±2.2	9.0±1.6	1465.9	$(4, 5, 6)^-$
39	5296.2±1.1	0.55±0.13			1487.8	
40	5287.6±1.3	0.31±0.09	5283.0±2.1	7.4±1.8	1496.5	

TABLE 1 (continued)

No.	This work		Resonance capture [a]		Final state	
	E_γ (keV)	I_γ per 1000 neutrons captured	E_γ (keV)	$\Sigma I_\gamma/E_\gamma{}^3$ [b]	(keV;	J^π)
41	5252.7±1.4	0.30±0.09			1531.3	
42	5245.3±1.1	1.27±0.27	5249.0±2.3	5.9±1.7	1538.7	
43	5240.2±2.0	0.27±0.15			1543.9	
44	5213.5±1.3	0.21±0.06			1570.6	
45	5189.6±1.2	0.36±0.09			1594.4	
46	5171.5±1.0	4.36±0.80	5175.2±2.4	10.6±2.0	1612.6	
47	5141.0±1.1	3.48±0.80	5143.3±2.4	11.8±2.1	1643.0	
48	5137.0±1.1	2.03±0.60			1647.0	
49	5118.7±1.1	1.00±0.21	5120.4±4.4	8.5±1.9	1665.4	
50	5111.8±1.6	0.42±0.12			1672.3	
51	5102.2±1.0	7.1 ±1.3	5105.8±2.4	15.2±2.3	1681.8	
52	5088.1±1.6	0.28±0.10			1695.9	
53	5081.0±1.1	0.77±0.17	5086.5±2.7	11.2±2.2	1703.0	
			5067.5±2.6	7.8±2.1		
54	5047.6±1.1	0.40±0.10			1736.4	
55	5031.7±1.0	1.28±0.25	5035.3±3.6	8.9±2.2	1752.3	
56	5014.7±1.0	0.80±0.16	5017.4±4.0	16.0±2.2	1769.4	
57	5004.6±1.0	2.60±0.49	5007.7±3.4	11.5±2.4	1779.4	
58	4997.1±1.1	0.79±0.17			1787.0	
59	4985.2±1.1	0.58±0.13			1798.9	
60	4968.8±1.0	4.13±0.78	4971.8±5.5	11.4±2.2	1815.2	
61	4962.5±1.0	1.62±0.33			1821.5	
62	4955.1±1.0	1.49±0.29	4959.1±4.9	5.6±2.2	1828.9	
63	4924.6±1.0	0.84±0.18			1859.5	
64	4914.6±1.0	2.45±0.47	4915.3±8.4	13.6±2.7	1869.4	
65	4908.5±1.0	2.08±0.41			1875.6	
66	4898.9±1.1	0.84±0.19	4901.7±7.9	10.3±2.6	1885.2	
67	4892.3±1.1	0.64±0.16			1891.8	
68	4877.4±1.0	0.89±0.19	4880.5±3.0	10.5±2.4	1906.6	
69	4868.4±0.9	3.2 ±0.6	4872.2±2.8	9.9±2.6	1915.6	
70	4862.0±1.2	0.69±0.17			1922.0	
71	4849.4±1.0	1.23±0.24	4852.7±3.2	7.4±2.5	1934.6	
72	4821.8±0.9	1.15±0.18	4825.8±3.2	7.4±2.5	1962.3	
73	4807.0±0.9	1.58±0.24	4812.3±3.3	9.8±2.7	1977.1	
74	4774.0±0.9	3.74±0.54	4778.0±5.7	27.2±4.0	2010.0	
75	4764.5±0.9	1.36±0.21			2019.5	
76	4742.5±0.9	2.26±0.34	4745.4±6.0	8.0±2.8	2041.5	
77	4734.5±1.1	0.59±0.13			2049.6	
78	4723.5±1.0	0.63±0.13	4729.1±4.0	11.5±3.3	2060.6	
79	4706.6±1.1	0.40±0.10			2077.4	
80	4699.0±0.9	2.14±0.31	4704.1±4.1	9.9±3.3	2085.1	
81	4682.8±0.9	1.20±0.19			2101.2	
82	4675.3±0.9	1.42±0.22	4680.9±4.0	5.6±2.9	2108.8	
83	4665.3±1.5	0.67±0.33			2118.8	
84	4661.4±1.4	0.77±0.33			2122.7	
85	4651.7±0.9	2.11±0.31	4658.4±4.0	7.5±3.0	2132.4	
86	4635.8±1.2	0.37±0.14			2148.3	
87	4624.0±1.0	1.19±0.21	4627.5±3.2	10.0±3.7	2160.0	
88	4616.0±1.2	0.76±0.18	4617.1±3.3	11.3±3.5	2168.0	
89	4610.0±1.1	0.86±0.20				
90	4597.0±0.9	2.02±0.32	4597.9±3.4	9.9±3.3	2174.1	
91	4588.4±0.9	1.85±0.29			2195.7	
92	4578.6±0.9	2.70±0.42	4583.9±3.4	10.2±3.2	2205.4	

[a]) Ref. [16]). [b]) In units of $10^{-3}\times$(photons per 100 neutrons captured $\times$ MeV^{-3}).

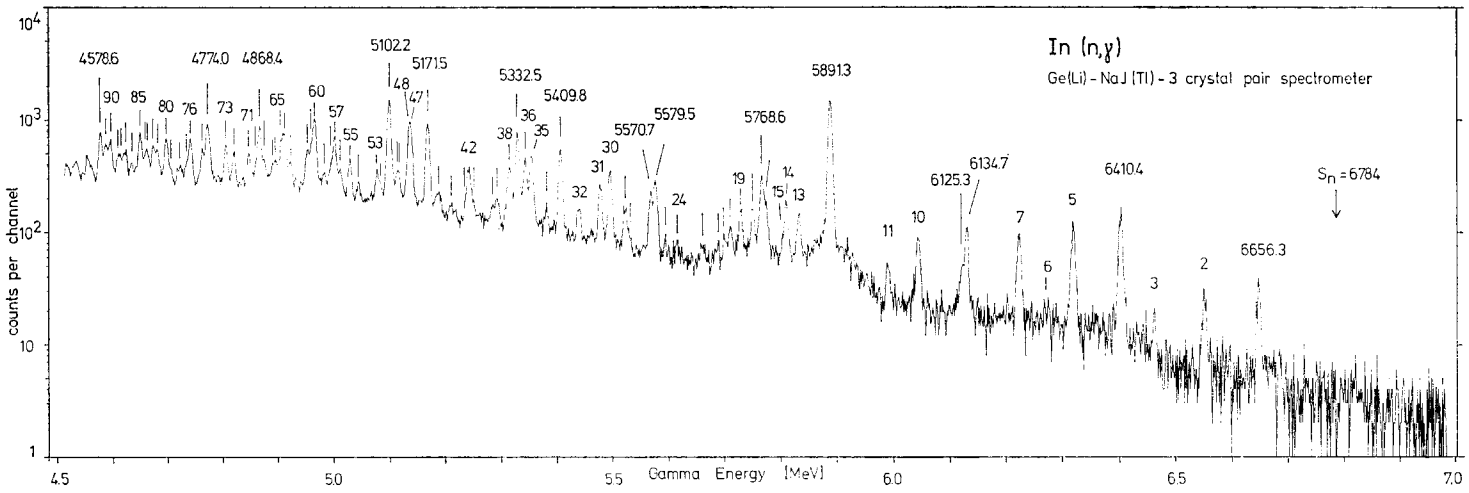

Fig. 1. High-energy γ-ray spectrum from the reaction In(n, γ) measured with a pair spectrometer. Numbers refer to table 1.

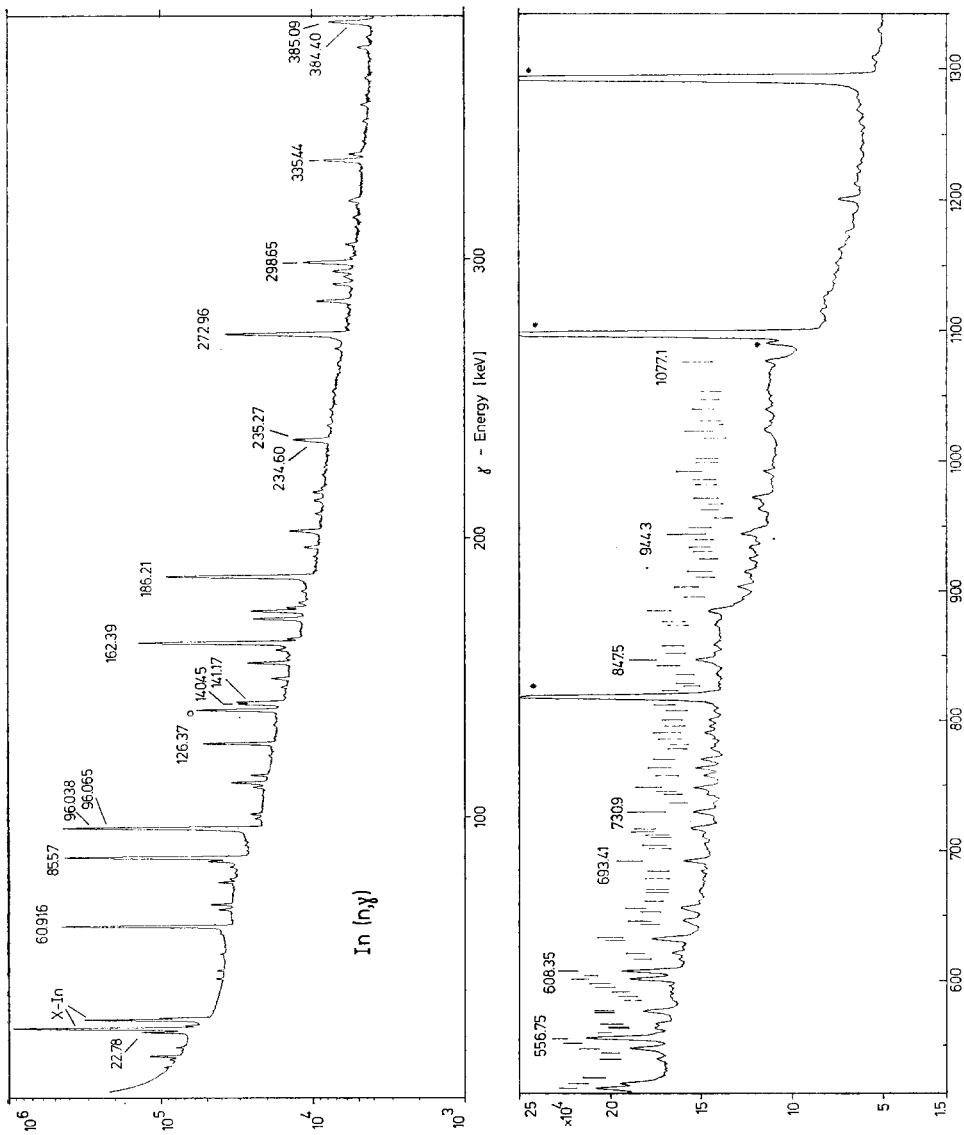

Fig. 2. Low-energy γ-ray spectra from the reaction In(n, γ) measured with a planar Ge(Li) detector (400 eV FWHM at 60 keV) (upper part) and with a 25 cm^3 five-sided Ge(Li) detector (2.5 keV FHWM at 1.3 MeV).

TABLE 2

Energies and intensities of low-energy γ-transitions from $^{115}In(n,\gamma)^{116}In$

No.	Present work		Leningrad group		Adopted values		Level depopulated [b]	Coincident transitions (no.)
	E_γ (keV) (δE_γ)	I_γ (‰) [a] (δI_γ)	E_γ (keV) (δE_γ)	I_γ (‰) [a] (δI_γ)	E_γ (keV) (δE_γ)	I_γ (‰) [a] (δI_γ)		
1	22.78 (5)	45 (15)			22.78 (5)	45 (15)	373	
2	42.15 (5)	1.3 (3)			42.15 (5)	1.3 (3)	893	9, 13, 23, 25?, 62, 69, 85?, 139
3	45.00 (5)	1.1 (3)			45.00 (5)	1.1 (3)	(1015)	
4	53.83 (10) [c]	0.3 (2)			53.83 (10)	0.3 (2)	(789)	
5	60.92 (5)	135 (40)	60.915 (1)	100 (10)	60.915 (1)	115 (20)	351	9, 13, 22, 23, 34, 37, 69, 85, 104A 106, 122, 135, 140, 156, 157, 162, 168, 184
6	76.75 (5)	2.8 (4)	76.757 (2)	2.6 (4)	76.757 (2)	2.7 (4)	366	71
7	82.32 (5)	1.0 (2)	82.312 (3)	0.9 (2)	82.312 (3)	0.9 (2)	508	13, 41, 46, 70
8	84.30 (5)	3.8 (6)	84.307 (2)	5.1 (6)	84.307 (2)	4.5 (6)	829	27, 55?, 62, 115
9	85.58 (4)	157 (11)	85.568 (2)	151 (15)	85.568 (2)	154 (11)	459	5, 13, 22, 23, 34, 37, 44?, 48, 51, 58, 69, 85, 101, 102, 106, 122, 135, 140, 156, 159, 168, 181?, 187, 191
10			85.947 (6)	1.3 (2)	85.947 (6)	1.3 (2)	875	41, 26?, 83?
11	90.15 (5)	0.38(15)	90.149 (4)	0.57(20)	90.149 (4)	0.47(15)	313	
12	95.41 (8)	6 (2)	95.378 (4)	4.3 (4)	95.378 (4)	4.3 (4)	761	95
13	96.05 (2)	179 (11)	96.038 (5)	66 (4)	96.038 (5)	68 (4)	555	5, 9, 22, 23, 27, 34, 37, 46, 51, 64, 68?, 69, 74, 80, 82?, 85, 90?
14			96.065 (5)	104 (6)	96.065 (5)	107 (6)	223	97, 102, 108, 113, 123?, 130, 143, 166, 174?, 179, 186, 189, 191, 197
15	99.50 (10)	1.1 (2)			99.50 (10)	1.1 (2)		
16	101.14 (10)	0.6 (3)			101.14 (10)	0.6 (3) [d]	(658)	9, 13?, 30, 35, 37, 122, 139
17	101.14 (10)	1.1 (5)			101.14 (10)	1.1 (5) [d]	1053	
18	108.3 (2)	0.15(10)			108.3 (2)	0.15(10)	(556)	
19	110.78 (5)	1.7 (2)	110.776 (4)	2.1 (4)	110.776 (4)	1.8 (2)		62?
20	112.00 (10)	1.4 (5)	112.080 (6)	1.9 (4)	112.080 (6)	1.7 (4)	761	41, 83
21	112.46 (5)	7.0 (7)	112.454 (3)	6.8 (6)	112.454 (3)	6.9 (6)	426	41
22	115.00 (4)	3.0 (3)	114.995 (3)	3.6 (4)	114.995 (3)	3.3 (3)	1008	9, 13, 20?, 34, 37, 85, 106
			121.971 (8)	1.3 (2) [c]				

23	126.370 (2)	24.7 (12)	126.370 (2)	26.8(15)	126.370 (2)	25.5 (12)	1019	5, 9, 31, 34, 37, 41?, 55, 62, 64, 68?, 69, 83?, 85, 97, 106, 115?, 131?, 139, 146
24	133.24 (8)	0.9 (3)			133.24 (8)	0.9 (3)	(791)	62, 98?
25	136.3 (2)	0.2 (1)			136.3 (2)	0.2 (1)		
26	140.46 (4)	12.3 (20)	140.454 (2)	14.7(15)	140.454 (2)	13.7 (15)	789	32, 41, 62?, 83, 131
27	141.17 (4)	13.7 (20)	141.169 (2)	16.4(17)	141.169 (2)	15.2 (17)	970	8, 13, 35, 43, 55, 62, 64, 80, 98, 115
27A	143.55 (10)	0.2 (1)			143.55 (10)	0.2 (1)		
28	146.57 (5)	1.2 (2)	146.522 (2)	1.1 (2)	146.522 (2)	1.2 (2)	[936]	41
29	149.70 (4)	4.0 (3)	149.668 (2)	4.5 (4)	149.668 (2)	4.0 (3)	[921]	36, 62?, 182
30	155.27 (2)	14.2 (20)	155.267 (3)	15 (2)	155.267 (3)	14.6 (20)	813	14?, 31, 46?, 50, 62, 96, 98
31	157.01 (5)	1.3 (2)	156.953 (3)	1.1 (2)	156.953 (3)	1.2 (2)	970	30
32	159.93 (4)	3.0 (5)	159.929 (4)	3.8 (4)	159.929 (4)	3.4 (4)	949	26, 41, 83
33	162.39 (2)	147 (10)	162.390 (3)	147 (8)	162.390 (3)	147 (10)	290	
34	163.81 (4)	2.2 (5)	163.806 (11)	2.8 (4)	163.806(11)	2.5 (4)	893	9, 13, 22, 23, 37
35	171.08 (3)	17.4 (15)	171.071 (6)	19 (2)	171.071 (6)	18.0 (15)	829	27, 43, 62, 96?, 98
36					173.44 (17) [d]	2.7 (11)	[1094]	29, 60?, 86
37	173.84 (4)	22 (3)	173.886 (6)	17 (2)	173.89 (3)	20 (3)	729	5, 9, 13, 22, 23, 29, 34, 159
38	175.10 (6)	5.0 (6)	175.063 (4)	5.7 (6)	175.063 (4)	5.3 (6)	[448]	23?, 62, 86?, 133?, 139?
39	176.84 (5)	1.9 (3)	176.823 (14)	1.9 (4)	176.823(14)	1.9 (3)		9?, 26, 41?, 55?, 100?
40	180.93 (6)	1.0 (2)	180.951 (21)	0.9 (2)	180.951(21)	1.0 (2)	970	26, 41, 83
41	186.21 (2)	138 (11)	186.207 (3)	138 (8)	186.207 (3)	138 (8)	313	10, 20, 21, 26, 32, 40, 43?, 48, 54, 61, 72, 81, 83, 105, 109?, 118, 125, 180, 217
42	193.50 (10)	0.6 (3)			193.50 (10)	0.6 (3)		62?
43	196.71 (3)	4.0 (5)	196.735 (5)	4.7 (6)	196.71 (3)	4.3 (5)	1167	8, 27, 35, 41, 54, 62, 80, 98, 153?
44					202.12 (8) [d]	1.0 (6)	1053	30, 62, 69, 98, 139
45	201.89 (10)	1.7 (5)	202.151 (16)	1.3 (4)	202.15 (2)	1.2 (4)	1015	
46	202.58 (5)	10.3 (11)	202.602 (6)	10.7 (6)	202.602 (6)	10.6 (6)	426	14, 90
47	208.89 (6)	1.8 (4)			208.89 (6)	1.8 (4)		
48	213.64 (5)	3.6 (5)	213.635(20)	2.6 (4)	213.635(20)	3.0 (4)	949	41, 105, 154
49	216.51 (5)	3.1 (5)	216.485 (25)	3.6 (4)	216.485(25)	3.4 (4)	(977)	20?, 41?, 83?
50	217.90 (10)	0.5 (3)	217.870 (30)	0.9 (2)	217.87 (3)	0.7 (2)	1031	30, 62
51	222.59 (9)	0.6 (3)	222.615 (30)	0.9 (2)	222.61 (3)	0.8 (2)	951	9, 13, 37
52	225.47 (10)	0.6 (3)	225.470 (30)	0.9 (2)	225.47 (3)	0.8 (2)	970	62
53	230.26 (9)	0.6 (3)	230.322 (35)	0.6 (2)	230.322(35)	0.6 (2)	[787]	
54	234.62 (5)	4.3 (13)	234.599 (6)	5.1 (6)	234.599 (6)	4.9 (6)	970	41, 154

TABLE 2 (continued)

No.	Present work		Leningrad group		Adopted values		Level depopulated [b]	Coincident transitions (no.)
	E_γ (keV) (δE_γ)	I_γ (‰) [a] (δI_γ)	E_γ (keV) (δE_γ)	I_γ (‰) [a] (δI_γ)	E_γ (keV) (δE_γ)	I_γ (‰) [a] (δI_γ)		
55	235.28 (4)	19.1 (16)	235.274 (4)	16.7 (9)	235.274 (4)	17.3 (9)	508	8, 22, 23, 27, 43, 62, 74, 80, 96?, 97
56	240.26 (7)	1.7 (3)	240.306 (40)	1.7 (4)	240.30 (4)	1.7 (3)	1031	62, 128, 180?
57	243.35 (15)	0.7 (2)	243.151 (27)	0.8 (2)	243.151(27)	0.7 (2)	1213	
58	246.09 (8)	1.4 (3)	246.095 (15)	1.9 (4)	246.095(15)	1.6 (3)	373	
59	252.65 (10)	0.6 (2)			252.65 (10)	0.6 (2)	(1082)	
60	262.20 (15)	2.4 (5)	262.220 (50)	1.5 (4)	262.22 (5)	1.9 (4)		
61	267.92 (8)	2.4 (6)	267.970 (34)	2.6 (4)	267.96 (3)	2.5 (4)		26?, 41, 83?, 120?
62	272.96 (2)	204 (10)	272.962 (2)	192 (9)	272.962 (2)	197 (9)	273	8, 23, 24, 27, 30, 35, 38, 43, 45, 47?, 55, 56, 59, 66, 74, 80, 84?, 87, 93, 96, 97, 98, 104, 107, 115, 124, 128, 133, 138, 142?, 146, 152, 160
63	282.79 (10)	1.1 (4)	282.820 (10)	1.1 (4)	282.820(10)	1.1 (4)	(791)	
64	284.86 (4)	26.8 (15)	284.898 (7)	27.1 (9)	284.898 (7)	27 (1)	508	14, 23, 27, 63?, 74, 80, 97
65			287.815 (65)	2.1 (4) [c]				
66	290.90 (4)	15.6 (8)	290.945 (15)	12.4 (6)	290.945(15)	13.6 (6)	1082	14, 62, 70, 90, 98, 128, 143
67	293.19 (15)	2.5 (8)			293.19 (15)	2.2 (8)	951	62?, 98
68	293.67 (4)	6.0 (10)	293.636 (12)	4.5 (4)	293.65 (3)	5.2 (10)	850	139
69	295.47 (3)	17.9 (11)	295.511 (27)	15 (2)	295.49 (3)	17.2 (11)	850	5?, 9, 13, 23, 44
70	298.66 (2)	59 (3)	298.654 (5)	49 (4)	298.654 (5)	55 (3)	426	66, 90, 148
71	299.5 (5)	1.3 (8)			299.5 (5)	1.3 (8)	666	6
72	300.25 (15)	3.2 (8)			300.25 (15)	3.2 (8)	949	41, 83
73	303.75 (30)	0.7 (2)	303.060 (50)	0.8 (2)	303.06 (5)	0.7 (2)	(729)	
74	305.14 (5)	6.0 (5)	305.125 (6)	6.2 (6)	305.125 (6)	6.1 (5)	813	14, 31, 55, 62, 64
75			306.818 (15)	0.8 (2) [c]				
76			307.965 (20)	0.6 (2)	307.965(20)	0.6 (2)		
			311.740 (85)	2.6 (4) [c]				
77	314.89 (10)	4.2 (4)	315.000 (30)	3.8 (4)	315.000(30)	4.0 (4)	666	5?, 12
78	318.45 (13)	3.1 (6)	318.560 (90)	2.1 (6)	318.52 (9)	2.6 (6)	875	
79	319.32 (13)	2.7 (10)	319.420 (90)	1.5 (6)	319.39 (9)	1.8 (6)	(977)	
80	320.95 (10)	9.1 (11)	320.902 (16)	8.3 (6)	320.902(16)	8.5 (6)	829	9, 14, 27, 55, 62, 64

81	321.71 (12)	4.0 (16)	321.642 (20)	5.1 (6)	321.642(20)	4.9 (6)	(970)	41
82	331.62 (20)	2.5 (5)			331.62 (20)	2.5 (5)	555	14
83	335.40 (4)	59 (4)	335.453 (13)	60 (4)	335.45 (2)	59 (4)	649	20, 26, 32, 40?, 41, 72
84					335.80 (4) [d]	2.0 (15)	893	138
85	337.68 (4)	15.6 (16)	337.712 (23)	17 (2)	337.70 (2)	16.1 (16)	893	9, 13, 22, 23
86	339.26 (10)	2.9 (5)			339.26 (10)	2.9 (5)	[787]	38
87	349.64 (10)	1.7 (4)			349.64 (10)	1.7 (4)	1094	62, 115?
88	358.93 (20)	1.9 (4)	358.756 (36)	1.3 (6)	358.756(36)	1.3 (6)	1008	
89			359.457 (40)	1.1 (6)	359.457(40)	1.1 (6)	(1253)	
90	365.10 (9)	3.3 (5)	365.150 (70)	4.0 (6)	365.13 (7)	3.6 (5)	791	14, 46, 70
91	368.61 (20)	0.8 (4)	368.556 (80)	0.9 (2)	368.56 (8)	0.9 (2)	(1303)	
92	370.3 (4)	0.5 (3)	369.906(100)	0.9 (2)	369.91 (10)	0.8 (2)	(1019)	
93	372.9 (2)	2.7 (5)			372.9 (2)	2.7 (5)	1031	62, 98
94	374.65 (20)	3.5 (10)			374.65 (20)	3.5 (10)		
95	375.97 (8)	16.6 (16)	375.947 (15)	18.1(11)	375.947(15)	17.6 (11)	666	12
96	379.61 (10)	6.2 (6)	379.570 (60)	5.7 (6)	379.58 (6)	6.0 (6)	[1193]	23?, 27, 30, 35, 47?, 55, 62, 74, 98
97	384.47 (8)	18 (4)	384.400 (50)	15.1(15)	384.42 (4)	15.5 (15)	893	14, 23, 55, 62, 64
98	385.08 (4)	58 (6)	385.093 (12)	75 (8)	385.092(12)	64 (6)	658	24, 27, 30, 35, 41?, 43, 47?, 50, 60?, 62, 96?
99	387.54 (45)	0.5 (3)	387.660 (70)	2.1 (6)	387.660(70)	0.5 (3)	761	
100	393.12 (12)	2.5 (3)			393.12 (12)	2.5 (3)	1286	9, 13, 97
101	394.71 (30)	1.5 (3)			394.71 (30)	1.5 (3)	949	9, 13
102	396.40 (10)	2.3 (3)	396.422 (26) [f]	4.5 (8)	396.42 (5)	2.3 (3)	951	9, 13
103	402.33 (29)	0.6 (3)			402.33 (29)	0.6 (3)	(850)	
104	410.51 (12)	4.6 (13)	410.387 (15)	7.0 (8)	410.39 (2)	3 (2) [d]	1286	62, 152
104A					410.39 (2)	3 (2) [d]	761	
105	422.17 (7)	8.8 (6)	422.197 (19)	13.6(13)	422.197(19)	8.8 (6)	736	41, 48, 54
106	433.705(35)	35.4 (16)	433.706 (14)	58 (4)	433.706(14)	35.4 (16)	893	5, 9, 22, 23, 58?
107	435.97 (30)	1.8 (5)			435.97 (30)	1.8 (5)	1094	
108	443.14 (8)	2.7 (6)	443.255 (40)	5.1 (4)	443.24 (4)	2.7 (6)	951	14, 55, 62, 64
109	448.22 (25)	1.4 (4)	447.35 (15)	1.9 (8)	447.35 (15)	1.9 (8)	761	
110	449.54 (35)	1.1 (4)	448.90 (10)	2.8 (8)	448.90 (10)	2.8 (8)		
111	452.59 (18)	1.3 (3)			452.59 (18)	1.3 (3)	(1008)	
112	458.61 (14)	3.5 (13)	458.30 (10)	3.4(13)	458.61 (14)	3.5 (13)	(1015)	
			459.39 (10)	2.4(11)				
113	465.40 (11)	3.5 (5)	465.525(100)	5.3 (6)	465.47 (8)	3.5 (5)	[1253]	62?
114	468.41 (17)	1.8 (4)	468.617(100)	4.7 (9)	468.56 (10)	1.8 (4)	1213	115
115	471.87 (5)	25.2 (13)	471.816 (19)	46 (7)	471.822(19)	25.2 (13)	745	8, 19?, 27, 43?, 52, 62, 87, 114

TABLE 2 (continued)

No.	Present work		Leningrad group		Adopted values		Level depopulated [b]	Coincident transitions (no.)
	E_γ (keV) (δE_γ)	I_γ (‰) [a] (δI_γ)	E_γ (keV) (δE_γ)	I_γ (‰) [a] (δI_γ)	E_γ (keV) (δE_γ)	I_γ (‰) [a] (δI_γ)		
116	474.42 (17)	4.1 (8)	474.215(100)	5.7(19)	474.27 (10)	4.1 (8)	1031	37?
117	475.87 (15)	9.0 (16)	475.875 (30)	14.5(43)	475.875(30)	9.0 (16)	789	32, 41
118	476.93 (25)	3.8 (16)	476.678 (60)	5.1(19)	476.69 (6)	3.8 (16)	[936]	9, 95?
119	485.57 (17)	2.6 (4)			485.57 (15)	2.6 (4)		
120	490.03 (30)	4.9 (5)			490.03 (30)	4.9 (5)	949	9
121					491.50 (50) [d]	2 (1)	1253	12
122	492.47 (5)	17.7 (13)	492.520 (14)	23 (2)	492.516(14)	17.7 (13)	951	5, 9, 17
123	497.64 (9)	2.7 (5)	497.68 (9)	5.8(11)	497.66 (9)	2.7 (5)	1053	9, 13
124					498.2 (2) [d]	1.5 (10)	771	
125					499.8 (2) [d]	1.5 (8)	813	41
126	515.74 (15)	4.6 (5)			515.64 (11) [d]	4 (1)	829	27, 41
127					515.94 (13) [d, e]	1.5 (10)	1071	9, 13
128	518.047(55)	17.5 (11)	517.938 (20)	25 (3)	517.95 (5) [d]	17 (2)	791	62, 66
129					518.1 (2) [d, e]	1.5 (10)	1167	41, 83
130	521.72 (7)	11.7 (11)	521.585 (45)	14 (3)	521.47 (2) [d]	1.0 (6)	745	14
131					521.62 (2)	11.2 (15)	649	20, 26
132	524.27 (50)	1.5 (6)			524.27 (50)	1.5 (6)	(1260)	
133	540.42 (13)	3.8 (5)	540.458 (24)	4.3(13)	540.45 (10)	3.8 (5)	813	62
134	545.48 (40)	2.5 (4)			545.48 (40)	2.5 (4)		30, 62?
135	548.72 (7)	11.6 (11)	548.685 (30)	21 (2)	548.69 (3)	11.6 (11)	1008	5?, 9, 49?
136	553.0 (5)	1.9 (4)			553.0 (5)	1.9 (4)		
137					555.45 (12) [d]	5 (3)	1204	41, 83
138					556.15 (1) [d]	10 (5)	829	27?, 62
139	556.71 (15)	21 (5)	556.747 (30)	38 (2)	556.8 (1)	20 (5)	557	23?, 68, 78
140	560.20 (18)	1.4 (13)	559.918(116)	7.5 (2)	560.00 (11)	4.1 (13)	1019	9
141	563.76 (32)	2.7 (8)	564.15 (10)	9.4 (2)	563.76 (32)	2.7 (8)	}	14, 41, 62, 98
142	565.03 (40)	2.0 (10)			565.03(40)	2.0 (10)	}	
143	567.64 (10)	5.6 (6)	567.745(114)	9.0(30)	567.69 (10)	5.6 (6)	791	14
144	573.74 (27)	1.7 (3)			573.74 (27)	1.7 (3)	1082	62?
145	576.21 (40)	2.7 (13)			576.21 (40)	2.7 (13)		
146	577.68 (12)	10.7 (13)	577.50 (5)	13.8(13)	577.53 (5)	10.7 (13)	850	23, 62
147	586.36 (23)	1.7 (3)			586.36 (23)	1.7 (3)	1400	30, 62?

148	589.40 (20)	2.6 (4)			589.40 (20)	2.6 (4)	(1015)		
149	592.88 (18)	2.8 (4)			592.88 (18)	2.8 (4)	(1019)		
150	596.63 (19)	3.2 (5)	597.37 (12)	4.1(15)	596.63 (19)	3.2 (5)			
151	599.46 (37)	1.4 (3)			599.46 (37)	1.4 (3)	[973]		
152	602.41 (15)	16 (2)	602.293 (35)	23.4(28)	602.30 (3)	16 (2)	875	62, 104	
153	605.22 (15)	3.2 (5)			605.22 (15)	3.2 (5)	(1031)		
154	608.346(19)	18.8 (27)	608.346 (19)	32 (3)	608.346(19)	18.8 (27)	736	48, 54?	
155	617.86 (35)	1.2 (3)			617.86 (35)	1.2 (3)	745		
156	622.51 (30)	3.5 (5)	622.63 (18)	10.2(34)	622.60 (18)	3.5 (5)	1082	9	
157	632.10 (13)	8.0 (16)	632.388(130)	14 (5)	632.25 (13)	8.0 (16)	1187	13	
158	634.00 (10)	7.7 (16)	634.062(110)	17 (6)	634.03 (10)	7.7 (16)	(761), (1008)		
159	645.62 (24)	2.4 (4)			645.62 (24)	2.4 (4)	1374	9, 37	
160	647.98 (17)	5.3 (7)			647.98 (17)	5.3 (7)	[921]	62	
161	654.92 (20)	3.0 (4)			654.92 (20)	3.0 (4)	(1400)		
162	657.43 (16)	7.2 (6)	657.14 (12) [f]	16.6(57)	657.26 (10)	7.2 (6)		14, 30?, 35	
163	662.16 (25)	1.3 (3)			662.16 (25)	1.3 (3)	(789)		
164	669.81 (41)	1.1 (3)			669.81 (41)	1.1 (3)	(892)		
165	672.22 (57)	0.7 (3)			672.22 (57)	0.7 (3)			
166	679.6 (5)	0.6 (2)			679.6 (5)	0.6 (2)	(1187)		
167	685.49 (27)	1.3 (3)			685.49 (27)	1.3 (3)	1343	62, 98	
168	693.38 (16)	7.3 (11)	693.430(125)	12 (2)	693.41 (12)	7.3 (11)		9	

No.	Present work		Level depopulated [b]	Coincident transitions	No.	Present work		Level depopulated [b]	Coincident transitions
	E_γ (keV)	I_γ (‰)[a]				E_γ (keV)	I_γ (‰) [a]		
169	703.01(28)	1.4 (3)			181	764.54(16)	8.8(11)		9?
170	706.22(25)	2.4 (4)	1451		182	771.00(16)	7.3(10)	771	14?, 29, 36?
171	711.27(22)	3.0 (5)			183	779.18(19)	4.0 (5)		
172	713.78(26)	3.2 (5)			184	782.71(24)	2.2 (4)		
173	717.14(31)	3.9(10)			185	788.44(21)	2.6 (4)	(1343)	
174	718.96(21)	6.8(14)	14?		186	791.51(60)	6.7 (7)	1015	14
175	730.85(16)	8.4(13)	(1286)		187	796.40(17)	4.4 (5)	(1303)	
176	737.16(26)	1.4 (4)			188	801.15(20)	4.6 (6)	1260	9
177	744.50(23)	4.0 (8)	(1253)	14, 62?	189	808.6 (10)	2.7(10)	1031	14
178	747.3 (8)	2.6 (8)	970	14?	190	814.07(27)	5.2(12)		
179	749.62(20)	8.3(17)	[973]	14	191	819.5 (2) [d]	5 (2)	1374	9, 13
180	758.89(17)	6.0(12)		41	192	822.63(29)	5.9(16)		

TABLE 2 (continued)

No.	Present work		Level depopulated [b]	Coincident transitions
	E_γ(keV)	I_γ(%) [a]		
193	827.7 (7)	0.6 (3)		
194	830.82(50)	1.1 (4)	(1204)	
195	837.01(23)	2.0 (4)		
196	844.24(24)	2.5 (4)		
197	847.53(16)	10.5(15)	1071	14
198	852.30(19)	3.1 (5)		
199	859.26(20)	2.6 (4)		
200	874.31(25)	2.4 (5)		
201	877.18(34)	1.6 (5)		
202	885.06(17)	5.4 (7)		14, 37?, 62?
203	896.06(46)	1.2 (5)	(1451)	
204	903.70(20)	6.4 (6)	(1031)	
205	910.79(26)	1.5 (3)		
206	915.32(17)	4.6 (5)	(1374)	
207	925.29(18)	3.7 (4)	(1053)	
208	930.60(24)	2.3 (4)		
209	934.11(17)	5.4 (6)		
210	939.60(18)	3.9 (5)		
211	944.27(16)	10.4(12)		
212	947.69(18)	5.5 (6)		
213	956.29(38)	0.9 (3)		
214	963.11(20)	4.9 (6)		
215	965.66(34)	2.7 (5)		
216	968.94(20)	4.3 (5)		
217	972.52(16)	9.0(10)	(1286)	
218	982.7 (5)	1.1 (4)		
219	986.04(45)	1.3 (4)		
220	992.10(17)	5.6 (6)	(1451)	
221	997.70(31)	1.6 (3)		
222	1001.51(33)	1.5 (3)		
223	1019.50(36)	1.5 (3)		
224	1023.37(25)	5.2 (8)		
225	1025.99(31)	3.3 (7)		
226	1030.54(26)	2.2 (4)		
227	1039.55(20)	3.6 (4)	(1167)	
228	1047.66(31)	1.2 (4)		
229	1053.24(33)	1.3 (4)		
230	1077.09(16)	8.6(12)	(1204)	

[a]) Only relative intensity errors are given; for absolute errors see text.
[b]) Notation of level assignment:
351: coincidence and singles data consistent with depopulation of the 351 keV level.
(791): assigned on the basis of energy difference only and assignment not safe.
[936]: assigned on the basis of energy difference only and feeding or de-exciting a doubtful level.
[c]) Transition probably in ^{114}In.
[d]) Transition found in a coincidence spectrum only.
[e]) Existence of the γ-line is doubtful.
[f]) Line width larger than in neighbouring lines.

2 MeV with the help of standard radioactive sources from IAEA, Vienna. The absolute intensity of the 162 keV transition between the second and the first isomeric states can be calculated because the isomeric cross section ratio [$\sigma_{m2}/\sigma_{tot} = 0.42 \pm 0.04$, ref. [27])], the K-conversion ratio [$\alpha_K = 1.15 \pm 0.09$, ref. [28])] and the K/LM ratio [1.6 ± 0.2, ref. [29])] are known fairly accurately. In this way, an absolute γ-intensity value of 147 ± 17 per 1000 neutron captures is obtained for the isomeric transition 162 keV. In column 2 of table 2 only relative intensity errors are given. Therefore, for absolute errors, the error of the calibration line has to be included as a systematic error.

In the range 1–4 MeV, the line density in the In(n, γ) spectrum is very high and there are no prominent lines (except from ^{116}In decay). Therefore, it did not seem worthwhile to us to extract energy values from this part of the spectrum. One also has to assume that, especially above 0.5 MeV, there are some multiple peaks in the spectrum which could not be resolved in our measurements.

We carried out three different γ-γ coincidence measurements:

(i) in the range (0–1, 0–1) MeV with two Ge(Li) detectors of 25 cm^3 sensitive volume and about 3 keV FWHM at 1.3 MeV;

(ii) in the range (0–0.75, 4.4–5.9) MeV with the same detectors. Because of the low coincidence rate and the unfavourable peak-to-background ratio on the high-energy side, only a few of these spectra coincident with high-energy peaks contain interesting information. In fig. 3, a few spectra of this kind are shown together with the high-energy coincidence sum spectrum;

(iii) in the range (0–0.6, 0–0.9) MeV. Here, the first detector of coincidence measurements (i) and (ii) has been replaced by a high-resolution 5 cm^3 planar Ge(Li) detector (1.1 keV FWHM at 122 keV).

Fig. 4 characterizes the coincidence (detection) efficiency achieved in the third coincidence experiment (90 h). These curves, which have been obtained from experimental values by means of the already known parts of the ^{116}In level scheme, have been useful in calculating the intensity of several γ-lines which could only be found in coincidence spectra, and in estimating whether a certain coincidence relationship of a given coincidence intensity could be detected or not.

In the last column of table 2, the numbers of all those transitions which are found in coincidence with the respective γ-line are given.

3.2. CONSTRUCTION OF THE LEVEL SCHEME

Apart from our own results, the very accurate crystal spectrometer data of Alexejev *et al.* [11]), the (d, p) measurements with a high-resolution magnetic spectrograph by Moorhead *et al.* [20]) and the neutron resonance capture study by Lone *et al.* [16]), have been especially helpful in the construction of the ^{116}In level scheme (fig. 11) and in the assignment of spins and parities to the levels.

The placement of the 126 keV line plays a key role in the construction of the level scheme. The spectrum coincident with this line and the spectrum coincident with the

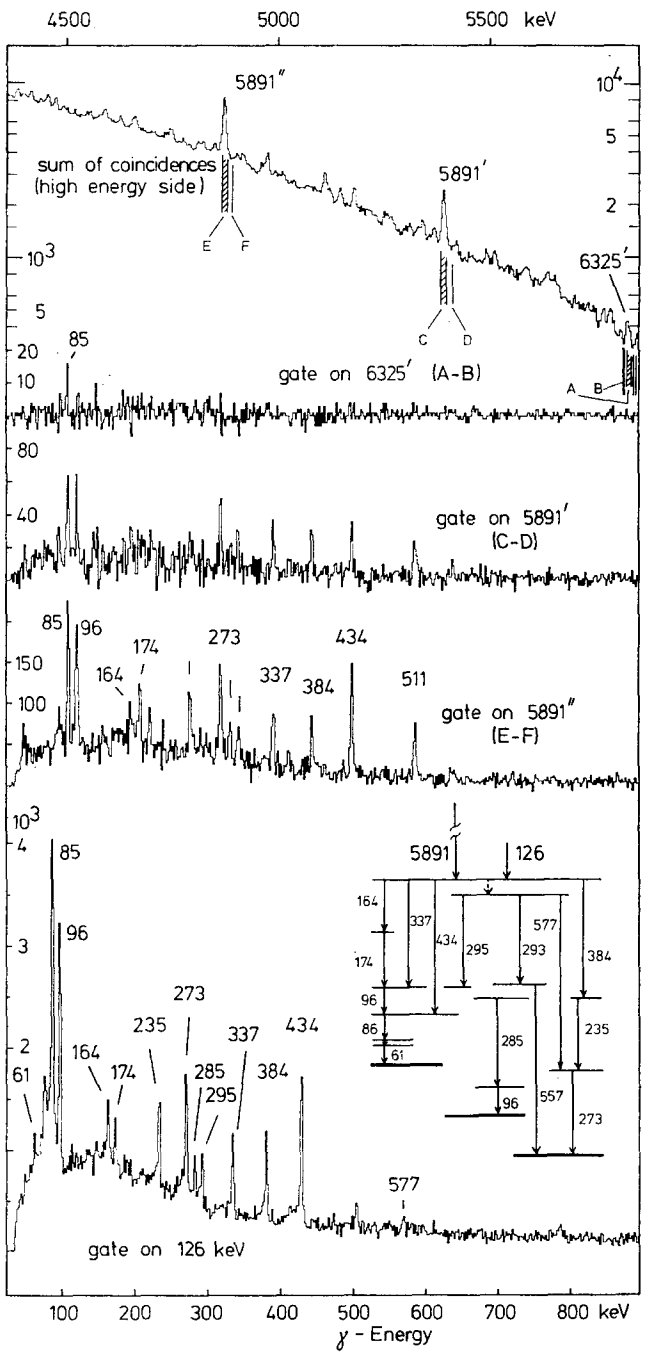

Fig. 3. Comparison of the γ-ray spectra coincident with the 5891 keV and 126 keV transitions, respectively.

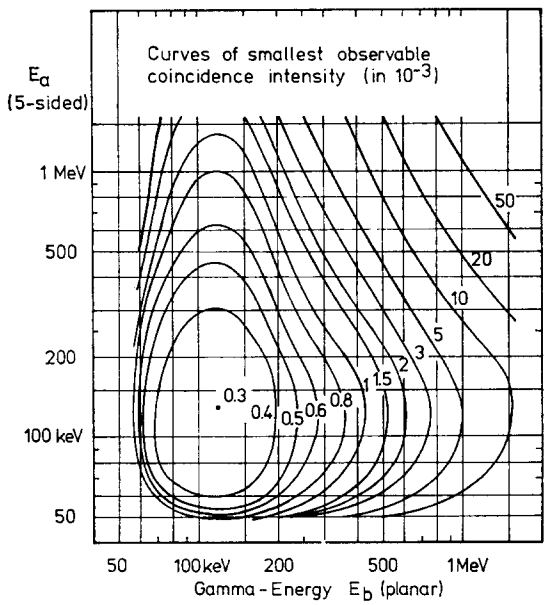

Fig. 4. Curves of smallest observable coincidence intensity (given in 10^{-3} per neutron capture) observed in an In(n,γ) 90 h γ-γ coincidence run using a 5 cm^3 planar Ge(Li) detector and a 25 cm^3 five-sided Ge(Li) detector.

strong primary transition of 5891 keV, which populates a level at 893 keV, seem to be identical (fig. 3).

It appears that the spectrum coincident with the 126 keV line can be explained without contradiction only if one assumes that the ground state and both isomeric states are appreciably populated from the 893 keV level. The decay to the ground state proceeds via cascade I [384.5, 235.3 and 273.0 keV] (fig. 8). From the level at 508 keV, casscade II [284.9 and 96.0 keV] decays to the first isomeric state. Cascade III [163.8, 173.9, 96.0, 85.6, 22.8 and 60.9 keV) connects the 893 keV level with the second isomeric state, in this way establishing levels at 729, 555, 459, 373, 351 and 290 keV.

To the levels at 555, 459 and 373 keV, primary transitions have been observed in thermal neutron capture; a primary transition to the 729 keV level has been observed only in resonance capture [16]). The spectra coincident with the different transitions of cascade III show that every cascade transition is in coincidence with every other cascade member (e.g. figs. 5 and 6). The 22.8 keV transition is placed above the 60.9 keV transition because the level at 351 keV, established in this way, has also been seen in the (d, p) study [20]). The whole cascade level construction is supported by a weak 246.08 keV transition, which is found in coincidence with the 85.6 keV line and fits exactly between the levels at 373 and 127 keV, the latter being the first isomeric state.

The levels at 223, 313 and 426 keV, which decay to the first isomeric state, are based

on energy sums and coincidence relationships and agree well with the (d, p) results [refs. [19,20])] and with the analog states in ^{116}Sn [ref. [18])]. The levels at 223 and at 313 keV are also populated by weak primary transitions. On account of the coincidence relationships between those transitions by which the levels at 223, 313 and 426 keV decay and other transitions, a number of higher-lying states have been established

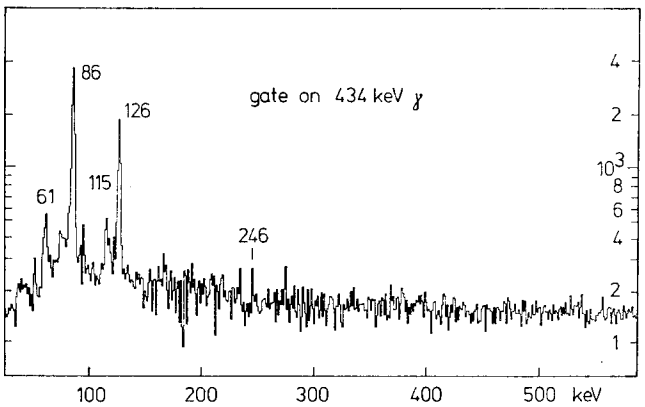

Fig. 5. Gamma-ray spectrum in coincidence with the 434 keV γ-line.

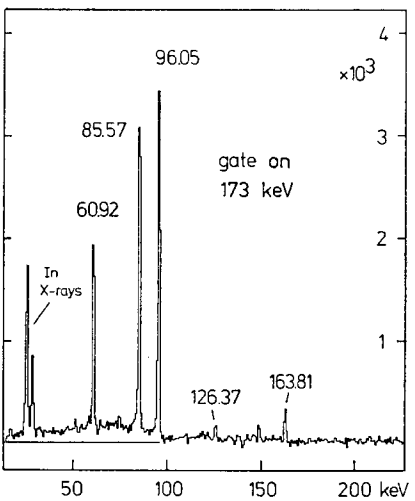

Fig. 6. Gamma-ray spectrum in coincidence with 173 keV. (This spectrum has been taken from a coincidence study of ^{114}In.)

(fig. 7): these are at 649, 736 (both also observed in (d, p) and populated by primary transitions), 761, 789, 791, 949 and 1082 keV.

The spectrum coincident to the 272.9 keV line (fig. 8) led us to assume the existence of several other energy states: those at 658, 745, 813, 829, 850, 875, 970 and 1031 keV. Most of them have not been observed in the (d, p) reaction and therefore, they might

be levels with a proton configuration different from the ^{115}In ground state. Several weak transitions have been placed between states of this group of levels and the group of levels which mainly decay to the first isomeric state.

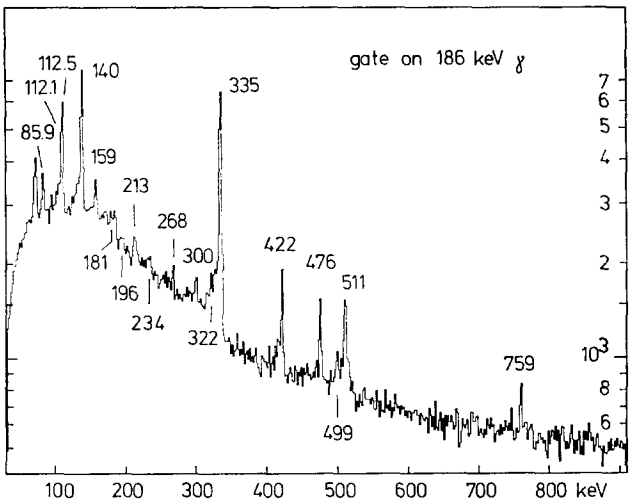

Fig. 7. Gamma-ray spectrum in coincidence with the 186 keV γ-line.

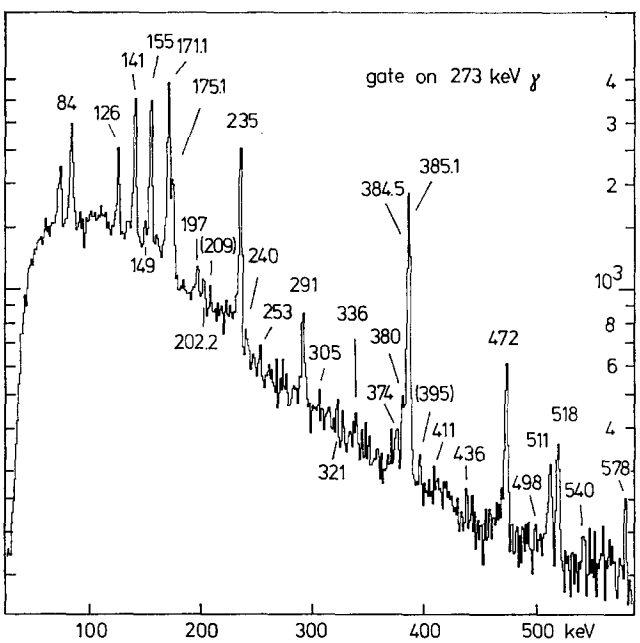

Fig. 8. Gamma-ray spectrum in coincidence with the 273 keV γ-line.

From the 850 keV level, which is populated by a 42.2 keV transition from the 893 keV level, a transition to a state of the negative-parity multiplet, the 555 keV state, is also seen.

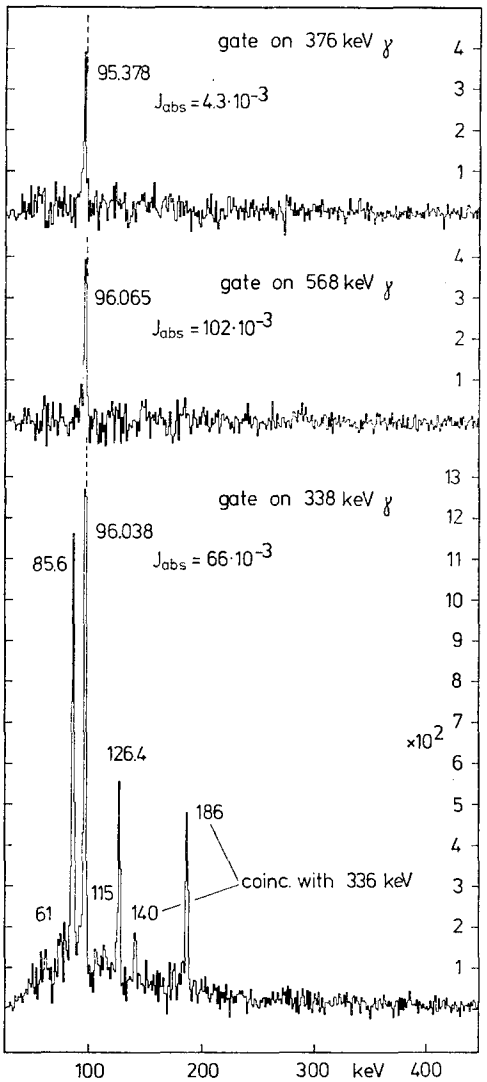

Fig. 9. Gamma-ray spectra coincident with the γ-transitions 337.7, 375.9 and 567.4 keV, which are coincident with different components of the complex 96 keV peak.

Besides the strong 272.9 keV line, only two other transitions to the ground state have been found, originating from new levels at 557 and 771 keV excitation energy. In both cases, only the ground state transition, depopulating the level, has been found. The 557 keV level is based on coincidences of the 557 keV line with the 294 and 319

keV transitions, both of which originate from levels also decaying to the 273 keV state.

The level at 771 keV is based on the coincidences of the 149.7 and 173.4 keV lines with the 771 keV line. Here, it is assumed that the 173.4 keV line, a transition found only in the coincidence measurements, populates a level at 921 keV, which decays to the 273 keV state by a 648 keV transition and to the 771 keV state by a 149.7 keV transition.

The peak at 96 keV (fig. 2) consists of 3 transitions. The energy difference between the strong lines of 96.038 and 96.065 keV is so small that they cannot be resolved with

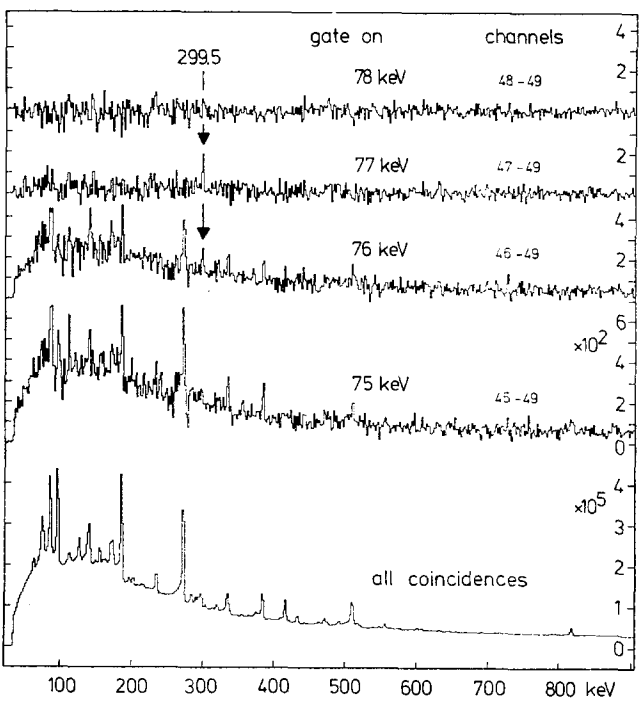

Fig. 10. Coincidence "slices" showing that a γ-line at 299.5 keV is in coincidence with the 76.8 keV transition. The contribution to the lower spectra, due to coincidence with lead X-rays, is rather similar to the sum spectrum of all coincidences.

a Ge(Li) detector. The weaker 95.378 keV line, which is coincident with the 375.9 keV one, can be satisfactorily separated from the other two lines in the coincident spectra (fig. 9). This important coincidence confirms a level at 665.6 keV, already seen in (d, p), which decays mainly to the second isomeric state at 289.7 keV. The cascade 299.5–76.757 keV is proposed as another decay branch of the 665.6 keV level. This cascade implies a level at 366.4 keV, already known from the (d, p) work. The transition 299.5 keV has been found only in the spectrum coincident with the 77 keV line (fig. 10).

In order to show how the line intensities observed in coincident spectra have been

used to extend the level scheme or to check the consistency of the existing part of the level scheme, the placement of the 175.063 keV line will be treated in more detail, because it led to the assumption of a new low-lying level at 448 keV. The relative intensities of the 175 keV transition in the singles spectrum and in a spectrum coincident to 273 keV line (fig. 8) are compared with the corresponding values of the 235.2 keV transition, which populates the 273 keV level directly. In the singles spectrum the intensity ratio of the two lines is 0.264 ± 0.040; the corresponding ratio in the spectrum coincident with the 273 keV transition is 0.198 ± 0.039. This result is compatible with the assumption that the 175 keV line directly populates the 273 keV level. If there were a transition between the 175 and the 273 keV transitions, it would be found in the spectrum coincident to the 175 keV line, unless its energy was either very small (< 50 keV) or rather large (> 1 MeV) (as seen in fig. 4, taking into account the intensity of the 175 keV line). Since neither is very probable, a level at 448 keV is tentatively proposed.

Four other levels below 1 MeV, at 787, 921, 936 and 973 keV, have not been safely established. All levels above 1 MeV (table 3) are based on primary transitions, with the exception of the levels at 1019 and 1193 keV.

The level energies and errors given in table 3 were obtained with a least-squares program, which fits the level energies to the energies of all unambiguously assigned transitions.

The consistent incorporation of a great number of the known transitions in the ^{116}In level scheme shows that a large fraction of the ^{116}In states lying below 1 MeV which are populated in the (n, γ) reaction with a measurable intensity are included in our level scheme.

In addition, table 3 shows that all states found in the (d, p) reaction below 900 keV [ref. [20])] are contained in our level scheme. We could not find a clear correspondence between our higher-lying levels, populated by primary transitions from the neutron capture state, and the (d, p) levels above 900 keV excitation energy. This may be understood by taking into account the high level density above 1 MeV which increases strongly with increasing excitation energy.

For the neutron binding energy of ^{116}In we obtained

$$B_n = 6784.2 \pm 1.2 \text{ keV}.$$

This value has to be compared with the corresponding values $B_n = 6781 \pm 3$ keV of Lone *et al.* [16]) and $B_n = 6779.5 \pm 1.5$ keV of Fubini *et al.* [8]). The significant discrepancy between our value and Fubini's value can be explained by the large difference of the level schemes used in calculating B_n.

3.3. SPINS, PARITIES AND POSSIBLE STRUCTURE OF THE ENERGY STATES IN ^{116}In

3.3.1. Ground state and isomeric states. Allowed β^- transitions of the ^{116}In ground state to the 0^+ ground state and the first excited 2^+ state of ^{116}Sn show that the ground state of ^{116}In has spin and parity $J^\pi = 1^+$. The spin and parity of the first

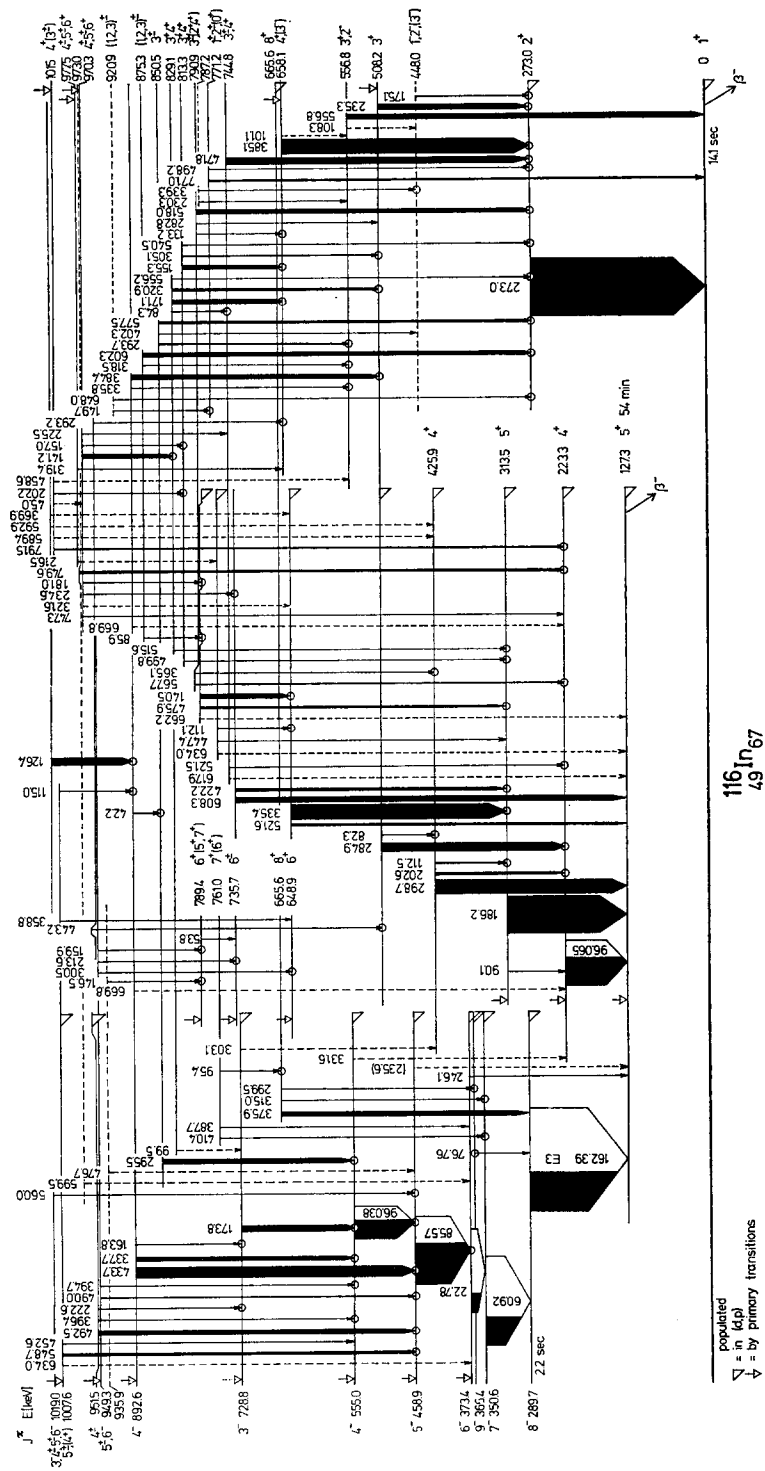

Fig. 11. Level scheme of ^{116}In up to about 1 MeV. A circle round the end of a γ-transition means that all observable coincidence relationships (according to fig. 4) between this transition and lower-lying transitions have been found. The widths of the transitions are proportional to their intensities.

TABLE 3

Energy levels and spin and parity assignments for ^{116}In

This work		(d, p) reaction [a])				
excitation energy (error) (keV)	J^π	excitation energy (keV)	l_n	J^π	S' [b])	S [b])
0	1^+	0	4	1^+	0.20	0.67
127.269 (5)	5^+	125	0	5^+	0.45	0.41
223.329 (5)	4^+	221	0	4^+	0.20	0.22
			2		0.12	0.13
272.962 (2)	2^+	273	0	$4^+, 5^+$	0.008	
289.660 (6)	8^-	288	5	8^-	1.07	0.63
313.475 (5)	5^+	313	2	5^+	0.56	0.51
			0		0.033	0.030
350.575 (6)	7^-	349	5	$5^-, 6^-, 7^-, 9^-$	0.90	0.60
366.417 (6)	9^-	366	5	$5^-, 6^-, 7^-, 9^-$	0.87	0.46
373.367(12)	6^-	373	5	$9^-, 10^-$	1.13	0.87
425.925 (5)	4^+	426	0	4^+	0.23	0.26
			2		0.43	0.48
448.026 (4) [c])	$1^-, 2^-(3^-)$					
458.935(12)	5^-	460	5	$5^-, 6^-, 7^-, 9^-$	0.92	0.84
508.233 (4)	3^+	508	2	3^+	0.57	0.81
554.972(13)	4^-	556	5	$3^-, 4^-, 5^-$	0.62	0.69
556.842(25)	$2^-, 3^+$					
648.899(10)	6^+	650	2	6^+	0.86	0.66
658.069 (6)	$4^+(3^-)$					
665.600(10)	8^+	666	5	$5^-, 6^-, 7^-, 9^-$	0.87	0.51
728.845(16)	3^-	729	5	$3^-, 4^-, 5^-$	0.57	0.81
735.686 (7)	$6^\pm$					
744.820 (6)	$3^\pm, 4^+$					
760.978(10)	$7^+(6^+)$	761	2(1)	2^+–7^+	0.18	
771.19 (10)	$1^\pm, 2^\pm, (0^+)$					
787.178(40) [c])	$(0$–$3)^\pm$					
789.353(10)	$6^+, (5^+, 7^+)$	790	2	2^+–7^+	0.14	
790.933(28)	$3^\pm(2^+, 4^+)$					
813.341 (6)	$3^+, 4^+$					
829.127 (6)	$3^+, 4^+$					
850.480(23)	$3^\pm$					
875.299(11)	$1^\pm, 2^\pm, 3^\pm$					
892.649(14)	4^-					
		913	2	2^+–7^+	0.16	
920.86 (10) [c])	$(1$–$3)^\pm$					
935.875(10)	$4^+, 5^\pm, 6^\pm, 7^-$					
949.284(10)	$5^\pm, 6^-$	951	1(?)	3^-–6^-	0.007	
951.450(16)	$4^\pm$					
970.295 (6)	$4^\pm, 5^\pm, 6^+$					
972.95 (19) [c])	$4^-, 5^\pm, 6^+$					
977.463(25)	$4^\pm, 5^\pm, 6^+$					
1007.644(14)	$5^\pm, (4^+)$	1007	1(?)	3^-–6^-	0.002	
1015.490(20)	$4^+, (3^\pm)$					
1019.019(14)	$3^-, 4^\pm, 5^\pm, 6^-$					
1031.206 (4)	$4^\pm, (5^+)$					

TABLE 3 (continued)

This work		(d, p) reaction [a]				
excitation energy (error) (keV)	J^π	excitation energy (keV)	l_n	J^π	S' [b]	S [b]
1052.605(50)	$4^\pm, 5^\pm, 6^+$					
1070.86 (15)	$4^\pm, 5^\pm, 6^\pm$					
1081.874(32)	$4^\pm, 5^+$					
1094.42 (9)	$4^\pm, 5^\pm, 6^+$					
1121.5 (14)	$4^\pm, 5^\pm, 6^\pm$					
1167.88 (16)	$4^+, 5^\pm, 6^\pm$					
1187.27 (12)	$4^\pm, 5^+$					
1192.922(38)	$(2\text{–}5)^\pm$					
1204.34 (12)	$5^\pm, 6^\pm$					
1213.36 (9)	$4^\pm, 5^\pm (3^-, 6^+)$					
1252.65 (9)	$(4\text{–}6)^\pm$					
1260.05 (19)	$(4\text{–}6)^\pm$					
1285.689(21)	$4^-, 5^-, 6^-$					
1304.43 (8)	$(4\text{–}6)^\pm$					
1343.45 (25)	$4^\pm, 5^\pm$					
1374.46 (15)	$4^-, 5^-, 6^-$					
1399.70 (22)	$4^\pm$					
1426.4 (10)	$(4\text{–}6)^\pm$					
1437.7 (10)	$(4\text{–}6)^\pm$					
1451.07 (23)	$4^\pm, 5^\pm$					
1465.9 (10)	$4^-, 5^-, 6^-$					

[a]) Ref. [20]).

[b]) These are related by the equation $S' = S(2J+1)/(2J_t+1)$, where J_t, J are the angular momenta of the target and final nuclei, respectively, and S the spectroscopic factors (S' is from ref. [20])).

[c]) Existence of level doubtful.

isomeric state (54.1 min) have been determined as 5^+ using atomic beam magnetic resonance. Heckmann *et al.* [28]) have measured the K-conversion coefficient of the 162 keV transition between the second and the first isomeric state, $\alpha_K = 1.15 \pm 0.09$, and found the multipolarity E3 for this transition (theoretical E3 value: $\alpha_K = 1.05 \pm 0.03$). Thus, the second isomeric state at 290 keV should have $J^\pi = 8^-$. It will be demonstrated below that this value is not in contradiction with the well-known high isomeric cross-section ratio of the second isomeric state [30–32]).

3.3.2. The $(\pi g_{\frac{9}{2}}^{-1}, \nu h_{\frac{11}{2}})$ *levels.* The position of the low-lying proton hole levels in ^{115}In and the quasineutron levels in ^{117}Sn are well known [3]). Using these level schemes, it is easy to estimate roughly at which excitation energies the various low-lying proton-hole states can be expected to lie (fig. 12). Most interesting are the low-lying negative-parity states which result from coupling a $g_{\frac{9}{2}}$ proton hole to an $h_{\frac{11}{2}}$ quasineutron. As fig. 12 shows, there are no other low-lying states with J^π between 7^- and 10^- which could mix with these states. Also, the lowest 5^- and 6^- states might have a rather pure configuration. The members of the $(g_{\frac{9}{2}}, h_{\frac{11}{2}})$ multiplet can be recognized by their orbital angular momentum $l_n = 5$ in the (d, p) reaction [20]).

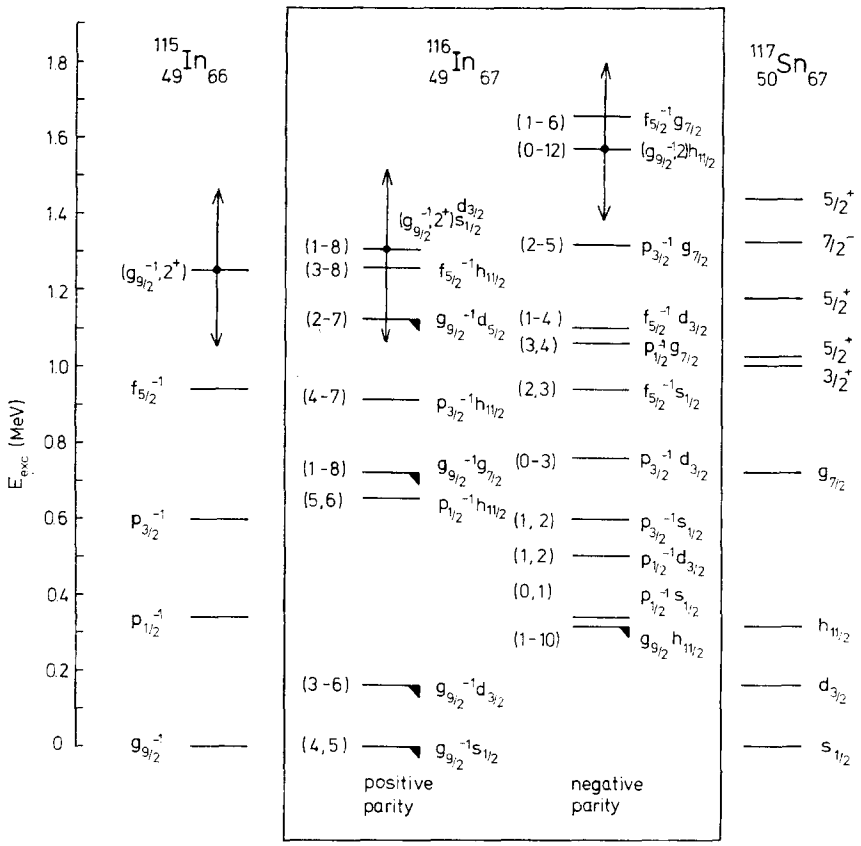

Fig. 12. Positions of low-lying proton-hole quasineutron states in ^{116}In constructed from ^{115}In and ^{117}Sn level schemes neglecting residual interaction.

By taking in consideration the decay of these states and the existence and strength of a primary population, the following classifications could be made: the second isomeric state ($l_n = 5$) can be regarded as the 8^- member of the multiplet. All three states at 373, 459 and 555 keV have $l_n = 5$ and are populated from the thermal capture state, which has predominantly $J^\pi = 5^+$. Because of their cascading decay, these states must have the spins $J = 6, 5, 4$ or $J = 4, 5, 6$ in the order 373, 459, 555 keV, respectively. The $l_n = 5$ state at 729 keV is not populated by primary transitions in thermal capture or from the 5^+ resonances at 1.46 and 9.1 eV, but rather clearly from capture in the 4^+ resonance at 3.86 eV [ref. [16])]. Therefore, this state is characterized by $J^\pi = 3^-$. The state at 555 keV, to which it decays, must have $J^\pi = 4^-$. The decay of the 373 keV (6^-) state to the 351 keV ($l_n = 5$) level and from there to the second isomeric state (8^-) suggests $J^\pi = 7^-$ for the 351 keV state.

There are only two other states below 1 MeV which have been characterized by $l_n = 5$ in ref. [20]): those at 366 and at 666 keV. Transitions from the 666 keV level to

the 366 keV level and to the 7^- and 8^- levels defined above have been found. The 366 keV state, itself, decays to the 290 keV level (8^-). Therefore, the characterization 666 keV (9^-) and 366 keV (10^-) would be possible. The transition from the 666 keV level to 351 keV (7^-) would then have E2 character and would compete with other M1 transitions (but the correct placement of this 315 keV transition is not proved by a coincidence relationship anyway).

We prefer the characterization 366 keV (9^-) and 666 keV (8^+) for the following reasons: (i) the decay of the 761 keV level ($7^+(6^+)$) to the 666 keV state; (ii) the atypical angular distribution of the 666 keV state, already noticed in the (d, p) work [20]); (iii) theoretical predictions for the positions of the 9^- and 10^- multiplet member states, using the positions of the states with $J^\pi = 6^-, 7^-$ and 8^- (see fig. 13); and (iv) the E1 character of the 376 keV transition [13]) from the 666 keV state to the 290 keV state. The 666 keV (8^+) state probably has $l_n = 4$.

The considerable configuration purity of the higher-spin negative-parity states may be seen from the weakness of E1 transitions from these states to lower-lying positive-parity states. In particular, the 246 keV transition from the decay of the 373 keV (6^-) level to 127 keV (5^+) is definitely established. This transition competes with the strong 23 keV M1 transition connecting the multiplet member states. Measured in Weisskopf units, this E1 transition is retarded by a factor of $(3\pm1)\times10^6$ compared to the M1 transition.

3.3.3. Other low-lying levels. Definite spin and parity values have already been proposed for the low-lying $l_n = 0$ and $l_n = 2$ states from the (d, p) work [20]). The classification of these states as

127 keV(5^+, $l = 0$), 223 keV(4^+, $l = 0, 2$), 313 keV(5^+, $l = 2, 0$),
426 keV(4^+, $l = 0, 2$), 508 keV(3^+, $l = 2$), 649 keV(6^+, $l = 2$),

is now supported by the strength of the transitions occurring between them: From the 508 keV(3^+) level, transitions could be found only to the 4^+ and not to the 5^+ states. The 6^+ level at 649 keV, on the other hand, decays only to the 5^+ states.

For two other $l = 2$ states at 761 and 789 keV, the possible range of spins could be confined much more than in the (d, p) work (see table 3).

For the spin and parity for the 893 keV state, $J^\pi = 4^-$ is proposed. This state is populated by strong primary transitions in the decay of most of the neutron resonances studied [16]); it decays to the 3^-, 4^- and 5^- levels and to the 3^+ level at 508 keV. Because of the strong primary transitions, which should have E1 character, negative parity is proposed for this level.

It is less easy to define spins and parities for the 273 keV state and for those levels which decay preferentially to this state and which have not been found in the (d, p) work [20]).

The 273 keV state is definitely not identical with an $l_n = 0$ ($J^\pi = 4^+, 5^+$) state found in the (d, p) work [20]) at this energy, because our 273 keV state decays exclusively to the ground state (1^+). It is very possible that there is a second state near 273 keV

with $l_n = 0$, covering a small peak of neutron transfer to our 273 keV state. However, we did not find any indication of such a 4^+ or 5^+ state, which should definitely be appreciably populated in the (n, γ) reaction.

According to refs. [13,29]), the multipolarity of the 273 keV transition is most probably M1. The transition from the 508 keV, 3^+ state and the fact that theoretically no other low-lying 1^+ state is to be expected implies $J^\pi = 2^+$ for the 273 keV state.

For the 850 keV level, $J^\pi = 3^+$ is proposed because it decays to the 555 keV (4^-), 273 keV (2^+) and 557 keV levels. The 557 keV level, which decays only to the ground state and not to the 273 keV state, which is, however, populated by a 335.8 keV transition from the 893 keV (4^-) level, should have $J^\pi = 3^+$ or 2^-.

The 175 keV transition, depopulating the 448 keV level, has E1 character according to ref. [13]). This level (assuming it really exists) should, therefore, have $J^\pi = 1^-, 2^-$ or 3^-, the smaller spins being more probable because of the low overall population of this level.

The 658 keV state is excited by primary γ-radiation. Since this state decays nearly exclusively to the 273 keV level, it should have $J^\pi = 3^-$ or 4^+. If 3^- were correct, both the 384.4 and 385.1 keV transitions would have E1 character. This should have been noticed in ref. [13]). This consideration renders $J^\pi = 4^+$ more probable.

With similar arguments for the remaining levels, the other spins and parities are restricted to the range given in table 3. Parts of these spin-parity ranges would be incorrect if any of the spins and parities already defined above proved to be wrong.

3.4. ISOMERIC CROSS-SECTION RATIOS

Thermal neutron activation cross sections for the isomeric states in ^{116}In have been measured and discussed by different authors [30-32]). This is because the strong population of the second isomeric state is in contradiction to the prediction of the statistical theory of isomeric cross-section ratios developed by Huizenga and Vandenbosch [ref. [33])], if one assumes $J^\pi = 8^-$ as spin and parity of the second isomeric state (see table 4).

TABLE 4

Isomeric cross-section ratios in ^{116}In from capture of thermal neutrons in ^{115}In

State	E_{exc} (keV)	J^π	$T_{\frac{1}{2}}$	$\left(\frac{\sigma_{act}}{\sigma_{tot}}\right)_{exp}$	$\left(\frac{\sigma_{act}}{\sigma_{tot}}\right)_{theor}$ [a])	
					for $J_{m2} = 8^-$	$J_{m2} = 5^-$
g	0	1^+	14.1 sec	0.21 ± 0.03	0.14–0.28	0.14–0.28
m_1	127.3	5^+	54.1 min	0.37 ± 0.04	0.61–0.82	0.28–0.49
m_2	289.7	8^-	2.16 sec	0.42 ± 0.04	0.04–0.11	0.37–0.44

[a]) From ref. [30]) calculated according to ref. [33]).

Alexander *et al.* [31]) proposed two different explanations for this discrepancy:

(i) Using the theory of Huizenga and Vandenbosch, one would conclude that the

spin of the second isomeric state is 5 or 6. The very large retardation for the 162 keV isomeric transition to the first isomeric state (5^+) would have to be explained, in this case, by the action of a *j*-selection rule on the transition between very pure shell-model states with configurations $(\pi g_{\frac{9}{2}}^{-1}, \nu h_{\frac{11}{2}})$ and $(\pi g_{\frac{9}{2}}^{-1}, \nu(s_{\frac{1}{2}}+d_{\frac{3}{2}}))$, respectively.

(ii) A similar *j*-selection rule could provide an efficient mechanism for directing the neutron-capture γ-ray cascade through the $(\pi g_{\frac{9}{2}}^{-1}, \nu h_{\frac{11}{2}})$ multiplet to its lowest-lying member, the isomeric 8^- state. The activation cross section represents, in this case, the cross section for the population of many of the multiplet members.

Our levels scheme shows that the second explanation is correct and that the reason for the breakdown of the statistical theory [33]) for ^{116}In can be found in the neglect of selection rules acting on transitions among low-lying states.

In ^{114}In, the isomeric cross-section ratios and the spins of the isomeric states are very similar to those in ^{116}In. Therefore, the same effects as in ^{116}In can be expected in ^{114}In.

4. Theoretical calculations

The Hamiltonian used in the theoretical calculations is

$$H = H_{\mathrm{p}}^{\nu} + H_{\mathrm{int}}^{(\pi,\nu)}, \tag{1}$$

where $H_{\mathrm{int}}^{(\pi,\nu)}$ is the interaction between the protons (π) and the neutrons (ν) and H_{p}^{ν} is the usual pairing Hamiltonian which is assumed to act only on the neutrons. Once the quasiparticle transformation is done, H_{p} can be written as

$$H_{\mathrm{p}}^{\nu} = \sum_{ljm} E_{lj}^{\nu} \beta_{ljm}^{+} \beta_{ljm},$$

$$E_{lj}^{\nu} = [(\varepsilon_{lj}-\lambda)^2 + \Delta^2]^{\frac{1}{2}}, \tag{2}$$

where ε_{lj} are the single-particle energies; λ, Δ are the chemical potential and the gap parameter respectively, and β_{ljm}^{+} is the creation operator of a neutron quasiparticle in a state *nljm*.

The residual proton-neutron interaction was assumed to be:

$$H_{\mathrm{int}}^{(\pi,\nu)} = \sum_{K=0,2,4} \kappa_K q_{K\mu}^{\pi *} q_{K\mu}^{\nu}, \tag{3}$$

where

$$q_{K\mu} = \sum_j r_j^2 Y_{K\mu}(\theta_i), \qquad K = 2, 4,$$

$$q_{00} = 1. \tag{4}$$

In this calculation the states of ^{116}In are described as a $g_{\frac{9}{2}}$ proton hole coupled to a neutron quasiparticle, i.e. the basis within which the Hamiltonian (1) is diagonalized is $|[\pi 0g_{\frac{9}{2}}]^{-1}, vnlj, J^{\pi}M\rangle$, where *vnlj* labels the neutron quasiparticle states.

The matrix elements of the proton-neutron interaction are

$$\langle[\pi 0g_{\frac{9}{2}}]^{-1}, \nu n_1 l_1 j_1, JM|H_{\text{int}}^{\pi,\nu}|[\pi 0g_{\frac{9}{2}}]^{-1}, \nu n_2 l_2 j_2, JM\rangle = -\kappa_0(U_{j_1}^2 - V_{j_1}^2)\delta_{l_1 l_2}\delta_{j_1 j_2}$$
$$+ \sum_{K=2,4}(-)^{\frac{9}{2}+j_1+J+1}\kappa_K(U_{j_1}U_{j_2} - V_{j_1}V_{j_2})\begin{Bmatrix} \frac{9}{2} & j_1 & J \\ j_2 & \frac{9}{2} & K \end{Bmatrix}$$
$$\times \langle 0g_{\frac{9}{2}}||r^2 Y_K||0g_{\frac{9}{2}}\rangle_p \langle n_1 l_1 j_1||r^2 Y_K||n_2 l_2 j_2\rangle. \quad (7)$$

In (7), $\langle \,||\,||\, \rangle_p$ denotes that the matrix element is taken between particle states.

In order to keep the κ_K as the only free parameters of this calculation, the E_{lj} and the factors U_{lj} and V_{lj} can be obtained from the neighbouring nuclei. It must be pointed out, however, that the one-particle transfer data [20]) show an anomalous population of the $h_{\frac{11}{2}}$ and $g_{\frac{7}{2}}$ levels in ^{115}Cd and ^{117}Sn. One possibility is, therefore, to use a set of single-particle energies which yields a reasonable description [34]) of ^{115}Cd. Another possibility is to assume that the lowest levels of ^{117}Sn are pure quasiparticle states. Thus from the corresponding energy spectrum and making use of the inverse-gap method, it is possible to obtain the quasiparticle energies E_{lj}, and the U_{lj}, V_{lj} and ε_{lj}.

In table 5, the different sets of single-particle energies which were obtained following these alternative procedures are summarized.

The strengths κ_2 and κ_4 in $H_{\text{int}}^{(\pi,\nu)}$ are determined by fitting to the energy differences of the 7^-, 8^- and 9^- states, while κ_0 is obtained using the energy of the 8^- state relative to that of the 1^+. The values obtained are given in table 5.

TABLE 5

Single-particle energies, BCS parameters and coupling constants for $H_{\text{int}}^{(\pi,\nu)}$

n	l	j	Set I [a])				Set II [b])				Set III [b])			
			ε_{lj}	E_{lj}	U_{lj}	V_{lj}	ε_{lj}	E_{lj}	U_{lj}	V_{lj}	ε_{lj}	E_{lj}	U_{lj}	V_{lj}
1	d	$\frac{5}{2}$	0	2.20	0.231	0.973	0	2.34	0.191	0.982	0	2.45	0.265	0.964
0	g	$\frac{7}{2}$	0.32	1.92	0.268	0.963	0.58	1.81	0.250	0.968	1.50	1.37	0.543	0.840
2	s	$\frac{1}{2}$	1.45	1.10	0.534	0.846	1.96	0.89	0.650	0.759	1.84	1.27	0.650	0.760
0	h	$\frac{11}{2}$	2.83	1.42	0.927	0.374	3.59	1.82	0.969	0.249	3.00	1.63	0.905	0.425
1	d	$\frac{3}{2}$	2.58	1.25	0.897	0.442	2.15	0.88	0.738	0.675	1.75	1.28	0.621	0.784
	Δ			0.9894				0.8783				1.2509		
	λ			1.7798				1.9823				1.9242		
κ_0 (MeV)				0.17244				0.30076				0.30063		
κ_2 (MeV/b^4)				−0.50081				−0.41135				−0.56357		
κ_4 (MeV/b^4)				−0.22622				−0.18581				−0.25457		

[a]) Obtained from the ^{117}Sn spectrum.

[b]) Taken from table 3 of ref. [34]). These are the values of ε_{lj} which give the best fit to the ^{115}Cd spectrum without anharmonic terms.

TABLE 6

Comparison of theoretically calculated and experimentally observed excitation energies of the $(\pi(g_{\frac{9}{2}})^{-1}, \nu h_{\frac{11}{2}})$ states

J	E_{exp}	E_{theor}
1		(2395)
2		(1847)
3	728.845	1242
4	554.972	746.57
5	458.935	461.519
6	373.367	370.433
7	350.575	350.575
8	289.660	289.660
9	366.417	366.417
10		1561.4

The states with spins $J = 7$, 8 and 9 are used to fit κ_2 and κ_4.

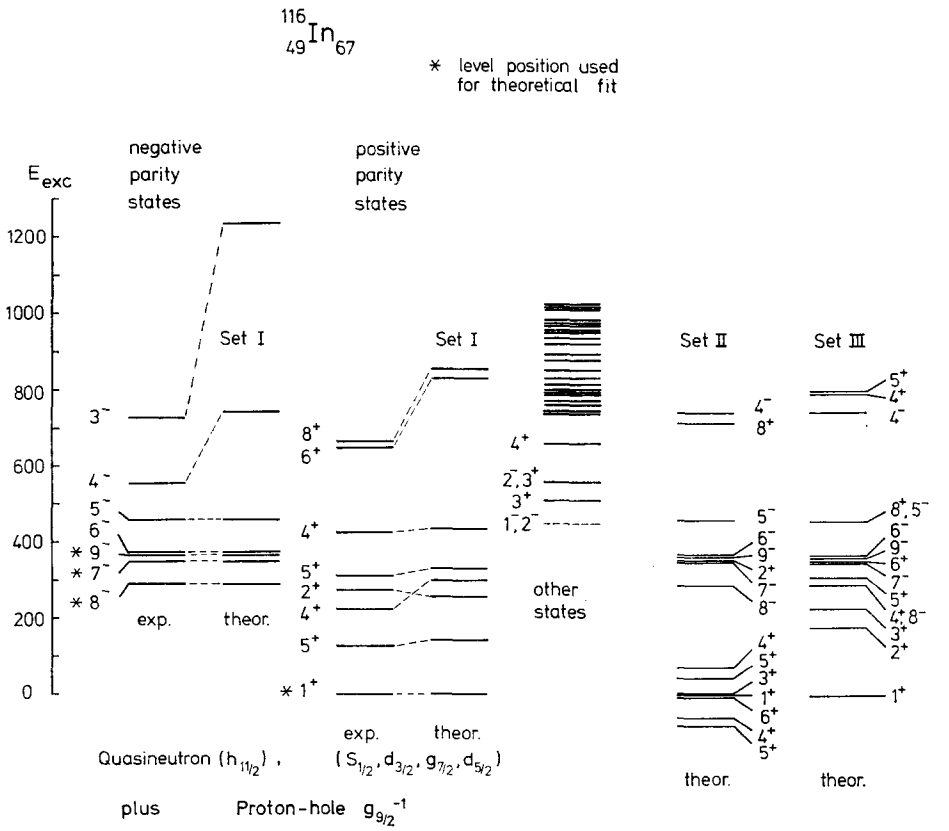

Fig. 13. Comparison of experimentally obtained and theoretically calculated excited states. For the three sets of single-particle energies used in the calculation, see table 5 and the text.

The energies of the negative-parity multiplet states are given in table 6. The position of the 10^- state, which has not been observed yet, should be predicted fairly well by this calculation.

The whole theoretical energy spectra are compared to experiment in fig. 13. From this comparison, it follows that all the states with a pure structure (such is the case of the 1^+, 8^+, and high-spin negative-parity states) are given reasonably well by the calculation.

On the other hand, all other states in which some configuration mixing is involved fail to be reproduced except for the calculation with the set I single-particle energies.

The theoretical branching ratios that were calculated with the wave functions corresponding to set I are compared to experiment in table 7. It is possible to conclude

TABLE 7
Branching ratios for electromagnetic transitions

Transitions	Branching ratios	
	exp.	theor.
$\frac{4_2 \to 4_1}{4_2 \to 5_2}$	1.54 ± 0.16	1.0
$\frac{4_2 \to 5_1}{4_2 \to 5_2}$	8.0 ± 0.7	7.3
$\frac{5_2 \to 4_1}{5_2 \to 5_1}$	$(3.4 \pm 1.1) \times 10^{-3}$	1.4

that within the present model, the description of complex states is not accurate enough to account for transition rates. Any improvement of these results would require the inclusion of either additional multipoles in (3) or more proton-hole states.

The main feature that can therefore be exploited in order to extract valid information about the proton-neutron residual interaction is the existence of certain levels having pure wave functions.

The value of κ_2 obtained is much larger than the one traditionally used in the description of quadrupole oscillations in doubly even nuclei, which is of the order of $-240A^{-\frac{5}{3}} = -0.089$ MeV/b^4, where b is the size parameter of the harmonic oscillator.

The anomalous values of κ_2 can have two possible interpretations. On the one hand, it may be that a stable deformation is present, as suggested by the existence of excited states in the odd In isotopes which can be interpreted as rotational bands. The occurrence of such deformations will be reflected, in this calculation, in a large value of the coupling constant, since spherical harmonic oscillator wave functions were used for the evaluation of the matrix elements of r^2. However, the quadrupole moment of the ground state of ^{116}In is experimentally known to be [35]) 9(2) fm^2 and the theoretical prediction is $(1 + e_{\text{eff}} - \frac{1}{2}(U_{\frac{7}{2}}^2 - V_{\frac{7}{2}}^2)e_{\text{eff}})$. It can therefore be seen that for reasonable values of e_{eff} it is possible to explain this value without introducing deformations.

On the other hand, the value of κ_2 can be understood † on the grounds of the presence of an isovector component [36]) in the quadrupole interaction:

$$H_Q = \kappa(0) Q^{T=0} \cdot Q^{T=0} + \kappa(1) Q^{T=1} \cdot Q^{T=1}. \tag{8}$$

This residual interaction gives rise to isoscalar and isovector collective modes both having excitations of particles either within an oscillator shell ($\Delta N = 0$) or across two ($\Delta N = 2$) such shells. The presence of the collective modes causes a renormalization of the strength of the bare interaction between two valence particles. This process can be pictured by the diagrams of fig. 14.

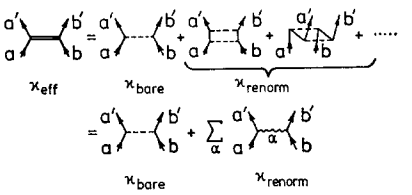

Fig. 14. Renormalization diagrams for the calculation of κ_{eff}.

The dotted lines represent a bare interaction and the wiggly line labelled α corresponds to all possible high-energy collective modes of excitation ($T = 0, 1$; $\Delta N = 0, 2$) which are different from those generated exclusively through the valence degrees of freedom.

From (8), it follows that

$$\kappa_{\text{bare}} = \kappa(0) + 4 t_z t_{z'} \kappa(1),$$

where t_z and $t_{z'}$ are the z-components of the isospins of the interacting valence particles. A relation can be established between $\kappa(0)$ and $\kappa(1)$, based on the isospin dependence of the central potential well [37]), namely $\kappa(1) = -3\kappa(0)$. Therefore, for identical particles $\kappa_{\text{bare}} = -2\kappa(0)$, being repulsive, and for the non-identical particle case $\kappa_{\text{bare}} = 4\kappa(0)$; however, if renormalizations are included, the strength acting between identical particles becomes barely attractive while $\kappa_{\text{eff}}^{\text{n.i.}} = 3.2\kappa(0)$.

The results obtained here for an effective neutron-proton quadrupole interaction are therefore consistent with these predictions. A further systematic analysis of other doubly odd nuclei is, however, desirable to confirm the idea that this effect is in fact due to the presence of an isovector term in the quadrupole force.

We are very grateful to Mrs. K. Demmel for her help in data reduction and in preparing the manuscript, and to the staff of the FRM for their services.

† G. G. Dussel and R. P. J. Perazzo want to acknowledge Prof. D. R. Bès for suggesting this interpretation of the anomalous values of κ_2.

References

1) M. Moinister, J. P. Schiffer and W. P. Alford, Phys. Rev. **179** (1969) 984
2) A. Bäcklin, B. Fogelberg and S. G. Malmskog, Nucl. Phys. **A96** (1967) 539;
V. R. Pandharipande, R. P. Sharma, K. G. Prasad and B. V. Thosar, Proc. Int. Conf. on nuclear structure, Tokyo, 1967, p. 175
3) E. U. Baranger, Advances in Nuclear Physics **4** (1971) 261
4) G. A. Bartholomew and R. B. Kinsey, Can. J. Phys. **31** (1953) 1025
5) L. V. Groshev, A. M. Demidov, V. N. Lutsenko and V. I. Pelekhov, Atlas of γ-ray spectra from radioactive capture of thermal neutrons, transl. J. B. Sykes (Pergamon Press, London, 1959)
6) V. Cojocaru, Acad. Rep. Populare Romine, Studii Ceretari Fiz. **14** (1963) 551
7) N. C. Rasmussen, quoted by L. V. Groshev *et al.*, Nucl. Data Tables **5** (1968) 48
8) A. Fubini, M. Giannini, E. Ivanov, D. Prosperi and V. Rado, Proc. Int. Symp. on neutron capture γ-ray spectroscopy, Studsvik, 1969 (IAEA, Vienna, 1970) p. 317
9) A. M. Berestovoi, I. A. Kondurov and Y. E. Loginov, Izv. Akad. Nauk SSSR (ser. fiz.) **30** (1966) 359;
Bull. Acad. Sci. USSR (phys. ser.) **30** (1967) 364
10) W. John and R. W. Jewell, Int. Conf. on nuclear physics with reactor neutrons, October, 1963, Argonne nat. lab. paper 11-8, ANL-6797 (1963) p. 143
11) V. L. Alexejev, D. M. Kaminker, E. G. Lapin, V. L. Rumyanzev and A. I. Smirnov, Program of the 20th meeting on nuclear spectroscopy and structure of the atomic nucleus, Leningrad, 1970, part 1, p. 69;
V. L. Alexejev, private communication
12) M. K. Balodis, V. A. Bondarenko, P. T. Prokof'ev and L. I. Simonova, Sov. J. Nucl. Phys. **1** (1965) 175
13) D. M. Kaminker, S. L. Sakharov and Y. L. Khazov, Program of the 21st meeting on nuclear spectroscopy and structure of the atomic nucleus, p. 66
14) A. M. Berestovoi, I. A. Kondurov and Y. E. Loginov, Program of the 20th meeting on nuclear spectroscopy and structure of the atomic nucleus, Leningrad, 1970, part 1, p. 70
15) J. E. Draper, C. A. Fenstermacher and H. L. Schultz, Phys. Rev. **111** (1958) 906
16) M. A. Lone, E. D. Earle and G. A. Bartholomew, Nucl. Phys. **A156** (1970) 113
17) R. E. Wahrer, J. D. King, A. H. Kukoc, P. J. Pan and H. W. Taylor, Nucl. Phys. **A154** (1970) 467
18) J. C. Thompson, K. Talbot and G. Perry, Nucl. Phys. **89** (1966) 209
19) S. A. Hjorth and L. H. Allen, Ark. Fys. **33** (1967) 121
20) J. B. Moorhead, B. L. Cohen and R. A. Moyer, Phys. Rev. **165** (1968) 1287
21) T. v. Egidy, K. Böning, A. Heidemann, L. Koester and D. Rabenstein, Research reactor utilization, IAEA-124, **1** (1970) 225
22) D. Rabenstein and H. Vonach, Z. Naturf. **26a** (1971) 458
23) D. Harrach, J. Glatz and K. E. G. Loebner, Proc. 6th seminar "Decus europe" (1970) p. 459
24) D. Rabenstein, Z. Phys. **240** (1970) 244
25) N. C. Rasmussen, Y. Hukai, T. Inouye and V. J. Orphan, MITNE-85 (1969) p.12
26) R. C. Greenwood and W. W. Black, Phys. Lett. **21** (1966) 702
27) M. D. Goldberg, S. F. Mughabghab, S. N. Purohit, B. A. Magurno and V. M. May, Neutron cross sections, vol. IIB, BNL 325 2nd ed., Suppl. 2 (1966)
28) P. H. Heckmann, K. Grubernator, J. Poyhonen and A. Flammersfeld, Z. Phys. **163** (1961) 451
29) P. F. Fettweis and E. C. Cambell, Compt. Rend. Congrès Int. de physique nucléaire, Paris, 1964, p. 492
30) K. F. Alexander, H. F. Brinckmann, F. Dönau and H. R. Kissener, Phys. Lett. **4** (1963) 302
31) K. F. Alexander, H. F. Brinckmann, C. Heiser and W. Neubert, Nucl. Phys. **A112** (1968) 474
32) W. Pönitz, Nucl. Phys. **66** (1965) 297
33) I. R. Huizenga and R. Vandenbosch, Phys. Rev. **120** (1960) 1305
34) D. R. Bès and G. G. Dussel, Nucl. Phys. **A135** (1969) 1
35) A. Winnacker, H. Ackermann, D. Dubbers, J. Mertens and P. von Blanckenhagen, Z. Phys. **244** (1971) 289
36) D. R. Bès and R. A. Broglia, private communication
37) A. Bohr and B. Mottelson, Nuclear structure (Benjamin, 1969) vol. 1, ch. 2